JGR Biogeosciences

RESEARCH ARTICLE
10.1029/2021JG006578

Key Points:

- Dissolved organic carbon concentration and dissolved organic matter (DOM) composition differ seasonally due to ice exclusion and microbial processing in the winter months
- Lake geomorphology is likely a major control for the overall lake DOM composition across the arctic tundra
- Tundra lake DOM composition differs in optical properties and heteroatomic content between coastal and inland lakes

Supporting Information:

Supporting Information may be found in the online version of this article.

Correspondence to:

M. R. Kurek,
mrk19f@my.fsu.edu

Citation:

Kurek, M. R., Frey, K. E., Guillemette, F., Podgorski, D. C., Townsend-Small, A., Arp, C. D., et al. (2022). Trapped under ice: Spatial and seasonal dynamics of dissolved organic matter composition in tundra lakes. *Journal of Geophysical Research: Biogeosciences*, *127*, e2021JG006578. https://doi.org/10.1029/2021JG006578

Received 11 OCT 2021
Accepted 23 MAR 2022

Trapped Under Ice: Spatial and Seasonal Dynamics of Dissolved Organic Matter Composition in Tundra Lakes

Martin R. Kurek[1], Karen E. Frey[2], François Guillemette[3], David C. Podgorski[4,5], Amy Townsend-Small[6,7], Christopher D. Arp[8], Anne M. Kellerman[1], and Robert G. M. Spencer[1]

[1]Department of Earth, Ocean and Atmospheric Science, Florida State University, Tallahassee, FL, USA, [2]Graduate School of Geography, Clark University, Worcester, MA, USA, [3]Department of Environmental Sciences, Research Center for Watershed-Aquatic Ecosystem Interactions (RIVE), Université du Québec à Trois-Rivières, Trois-Rivières, QC, Canada, [4]Ion Cyclotron Resonance Facility, National High Magnetic Field Laboratory, Tallahassee, FL, USA, [5]Department of Chemistry, Chemical Analysis & Mass Spectrometry Facility, Pontchartrain Institute for Environmental Sciences, University of New Orleans, New Orleans, LA, USA, [6]Department of Geology, University of Cincinnati, Cincinnati, OH, USA, [7]Department of Geography, University of Cincinnati, Cincinnati, OH, USA, [8]Water and Environmental Research Center, University of Alaska Fairbanks, Fairbanks, AK, USA

Abstract Arctic lakes store, modify, and transport large quantities of carbon from terrestrial environments to the atmosphere; however, the spatial and temporal relationships between quantity and composition of dissolved organic matter (DOM) have not been well characterized across broad arctic regions. Moreover, most arctic lake DOM compositions have been examined during the ice-free summer, whereas DOM cycling between the ice-covered winter months and summer have not been addressed. To resolve these spatial and seasonal uncertainties in DOM cycling, we sampled a series of arctic lakes from the North Slope of Alaska across a latitudinal gradient in the winter and summer over 3 years. Samples were analyzed for dissolved organic carbon concentration and DOM composition was characterized using optical and fluorescence properties combined with molecular-level analysis using Fourier transform-ion cyclotron resonance mass spectrometry. Tundra lake DOM properties including aromaticity and molecular stoichiometries were similar to other northern high-latitude lakes, but optical parameters related to aromaticity and molecular weight were greater in major arctic rivers and in coastal lakes in the North Slope region. DOM composition was highly seasonal, with ice exclusion concentrating microbially processed DOM in the winter water columns, potentially influencing DOM cycling the following summer. However, the greatest variations in DOM composition were related to lake depth and likely other physical features including morphology and bathymetry. As the Arctic warms, we expect changes in hydrology and ice cover to enhance under-ice microbial DOM processing, early summer photodegradation, and ultimately carbon fluxes to the atmosphere after ice-out.

Plain Language Summary Arctic lakes contain large amounts of both inorganic and dissolved organic carbon (DOC) that is stored, processed, and transferred to the atmosphere. This cycling has been enhanced by recent arctic warming via anthropogenic climate change, making the fate and distribution of these different pools uncertain on both seasonal and spatial scales. We demonstrate that the amount of DOC and the composition of dissolved organic matter (DOM) vary significantly across tundra lakes between summer and winter months when the lakes are entirely covered by ice. Furthermore, these seasonal trends are consistent across the North Slope of Alaska with lakes closer to the coast of the Arctic Ocean differing in bulk optical and molecular-level properties, suggesting DOM is supplied by different sources and influenced by maritime effects. Finally, while seasonality was an important factor in explaining DOM compositions across the tundra, the greatest differences between lakes were attributed to other factors, likely related to the variations in lake geomorphology including lake depth and area across the region. As temperatures and precipitation change across the Arctic are expected, lake morphology will respond to a thawing landscape and influence the composition of DOM as well as how it is cycled from lakes to the atmosphere.

1. Introduction

High-latitude arctic systems encompass approximately 25% of the Earth's vegetated land surface and store between 1,400 and 1,850 Pg carbon in soils and permafrost that can be mobilized to the atmosphere as greenhouse

gases (McGuire et al., 2009; Olefeldt et al., 2016; Schuur et al., 2015) as well as across inland waters including lakes and rivers (Cole et al., 2007; Drake et al., 2018; Kling et al., 1991; Stackpoole et al., 2017; Tranvik et al., 2009). Since the late twentieth century, increase in arctic surface temperatures has outpaced global averages by two-to three-fold, and it is projected to increase further owing to anthropogenic climate change (Collins et al., 2013). Increased warming across northern high-latitudes is predicted to release 5%–15% of carbon from soils and permafrost into the atmosphere this century (Schuur et al., 2015) and indirectly disrupt ecosystem carbon balance through changes in precipitation patterns, hydrology, and vegetation (Anderson et al., 2017; Arp et al., 2010; Jorgenson et al., 2006; Schuur et al., 2015; Wendler et al., 2017). These disruptions have profoundly altered the arctic landscape and resulted in thermokarst degradation and lake expansion (Abbott et al., 2015; Jones et al., 2011; Jorgenson et al., 2006; Olefeldt et al., 2016), which have been identified as hotspots for carbon cycling and emissions of greenhouse gases to the atmosphere as well as transport to the Arctic Ocean (Bogard et al., 2019; Hastie et al., 2018; Kling et al., 1991). With continued warming, many of these lakes are also experiencing changes to ice cover, such as ice thinning and variations in the time of ice-out (Arp et al., 2012), which will influence internal cycling and aquatic carbon storage between seasons. Both thermokarst expansion and shifting lake ice cover will impact the hydrologic connectivity of the arctic landscape between soils, aquatic systems, and the Arctic Ocean with implications for the feedback between greenhouse gas emissions and ecosystem carbon balance (Ducharme-Riel et al., 2015; Frey & McClelland, 2009; Hastie et al., 2018; Tank et al., 2012).

Climate change will also impact the distribution and transfer of other carbon pools, including freshwater dissolved organic carbon (DOC) and dissolved organic matter (DOM). DOM is a highly complex mixture of organic compounds composed of various terrestrial (allochthonous) and internally produced (autochthonous) sources, representing an important intermediary in the aquatic carbon cycle (Battin et al., 2009). The source of DOM impacts its functionality and how carbon travels through aquatic ecosystems (i.e., its role, processing, and fate) to the atmosphere. Biolabile DOM is often responsible for aquatic energy transfer and regulating food webs by serving as a reactive carbon and nutrient source for heterotrophs, while aromatic DOM can attenuate light through the water column, impacting primary productivity and CO_2 fixation (del Giorgio et al., 1994; Koehler et al., 2014; Solomon et al., 2015).

Freshwater DOM is an important component in the arctic carbon cycle, both in terms of land-to-ocean transfer and direct mineralization (Allesson et al., 2020; Bogard et al., 2019; Mann et al., 2016; Spencer et al., 2008). For instance, the annual DOC flux from arctic rivers to the ocean is estimated to range from 33 to 40 Tg (McGuire et al., 2009; Spencer et al., 2009) and incorporates DOM from a variety of terrestrial sources, including vegetation, soils, and permafrost that varies with seasonal discharge (Mann et al., 2016; Spencer et al., 2008; Wologo et al., 2021). In contrast, studies of DOC transfer and DOM composition between the landscape and freshwater arctic systems are less common and have made upscaling to the regional-level difficult due to the heterogeneities in landscape and climate across the pan-Arctic (Brown et al., 1997; Olefeldt et al., 2016; Stackpoole et al., 2017). While DOM composition and carbon dynamics have been well characterized across many separate arctic and boreal regions (Breton et al., 2009; Frey et al., 2016; Johnston et al., 2020; Kellerman et al., 2020; Osburn et al., 2017; Wauthy et al., 2018), their roles in governing aquatic carbon balance and future outlook vary by region (Bogard et al., 2019; Frey & McClelland, 2009; Hastie et al., 2018; Tank et al., 2011) with many areas in the Arctic, such as tundra ecosystems, underrepresented. Several studies across the Alaskan tundra have revealed the importance of these lakes as sources of atmospheric greenhouse gases (Elder et al., 2018; Kling et al., 1991; Townsend-Small et al., 2017), while other smaller scale studies have highlighted the landscape connectivity from headwater streams to lakes and how biolabile and photolabile DOM is processed during transport (Cory et al., 2007; Michaelson et al., 1998). However, the relationship between aquatic DOM composition and its role in carbon cycling across these regions has still not been fully resolved.

The inherent complexity of DOM benefits from complementary analytical techniques to characterize its functionality and for inferring its reactivity and stability. DOM composition has been characterized using bulk optical properties to determine its chromophoric dissolved organic matter (CDOM) content and fluorescence spectroscopy to identify molecular components in fluorescent dissolved organic matter (FDOM; McKnight et al., 2001; Spencer et al., 2008; Stubbins et al., 2014). The molecular-level properties of DOM composition have also been investigated using Fourier transform-ion cyclotron resonance mass spectrometry (FT-ICR MS) revealing differences in sourcing (Johnston et al., 2019; Kellerman et al., 2020), photolability (Gonsior et al., 2013; Stubbins et al., 2010), microbial processing (D'Andrilli et al., 2015; Spencer et al., 2015; Wologo et al., 2021), and

quantitative relationships between heteroatoms (Kurek et al., 2020; Poulin et al., 2017). Though DOM is ubiquitous in global freshwaters, its role will be increasingly important in the northern high-latitudes as reduced carbon from permafrost thaw becomes more susceptible to mineralization.

The winter period has received growing attention as an important contributor to arctic CO_2 fluxes from soil decomposition and is expected to increase with warming (Natali et al., 2019). In aquatic systems, this period is critical as large fluxes of greenhouse gases that have been trapped under the ice are emitted into the atmosphere during ice-out (Ducharme-Riel et al., 2015; Elder et al., 2018; Townsend-Small et al., 2017) and pulses of preserved DOM, that have been accumulating during the winter, are transferred into lakes driving summer carbon cycling (Johnston et al., 2020; Shatilla & Carey, 2019; Wickland et al., 2012). However, there is still limited knowledge concerning the composition and mineralization potential of organic matter, both temporally and spatially (Denfeld et al., 2018). For instance, regional arctic DOM cycling has mostly been studied during the ice-free period (e.g., Bogard et al., 2019; Johnston et al., 2019; Lapierre & Del Giorgio, 2014; Wauthy et al., 2018) while the extent of seasonal cycling between winter and summer remains unknown. Some studies have investigated the DOM composition of arctic lakes during the winter revealing differences between DOC and CDOM quantity (e.g., Belzile et al., 2002; Johnston et al., 2019; Santibañez et al., 2019); however, the coverage of lakes across the Arctic is sporadic, often focusing on isolated study sites at a single time point. Consequently, the spatial distributions of ice-free and under-ice lake DOM composition have not been thoroughly resolved including their responses to biogeochemical drivers and gradients in air and water temperatures. Therefore, we analyzed multiyear DOC concentration and DOM composition, including absorbance, fluorescence, and FT-ICR MS properties, across the Alaskan tundra following two north–south transects. Our goal was to compare DOC concentration and DOM composition in tundra lakes between the open water and ice cover across multiple sampling years to identify the potential spatial and seasonal drivers that influence carbon dynamics across this region.

2. Methods

2.1. Study Site and Field Sampling

Lakes were sampled from the North Slope of the Alaskan tundra (Figure 1). This area is characterized by shrub-like vegetation, flat terrain, and continuous permafrost (Brown et al., 1997) with thaw ponds and thermokarst lakes covering over 22% of the landscape (Hinkel et al., 2003). Elevation gradually decreases northward across the Alaskan coastal plain (Zhang et al., 1996) and is accompanied by a shift in sediment from aeolian silt to aeolian sand and glaciomarine deposits near the coast (Elder et al., 2018; Hinkel et al., 2005). Lake surfaces in this region remain frozen for 8 to 9 months of the year (Hinkel, Lin, et al., 2012) with the dates of surface ice break-up (ice-out) ranging from early June to mid-July depending on late spring temperature, lake depth, surface area, and distance from the coast (Arp et al., 2015). We sampled 10 lake groups from 2012 to 2014 during ice cover (April) and in the ice-free season (August) spanning two north–south transects from Toolik to Utqiagvik (formerly "Barrow"; Figure 1). Hereafter, we denote samples collected during ice cover as "winter" and those from the ice-free period as "summer." The lakes were part of the NSF-funded Circumarctic Lakes Observation Network (CALON) project and have been part of several biogeochemical studies involving greenhouse gas fluxes and inorganic geochemistry (e.g., Elder et al., 2018; Hinkel et al., 2017; Townsend-Small et al., 2017).

We sampled 81 individual lakes, of which 55 were sampled each year from 2012 to 2014 (see Supporting Information) using methods outlined in Townsend-Small et al. (2017). In the summer, lakes were accessed directly via floatplane or by road followed by an inflatable zodiac. In the winter, lakes were accessed by a snowmachine, and water samples were collected after drilling through the ice cover of lakes that were not frozen solid with bedfast ice (i.e., water frozen all the way to the lakebed). A YSI Model 63 sensor was used to measure in situ pH, specific conductivity (SpC), and dissolved oxygen (DO) at the lakes. Chlorophyll-*a* concentration was measured using a Turner Designs Trilogy Fluorometer upon return from the field. Summer water samples were collected at 0.5 m depth while winter samples were collected just below the ice layer. All water samples were syringe filtered through precombusted (450°C, >4 hr) Whatman GF/F filters (0.7 μm) into acid-rinsed high-density polyethylene (HDPE) bottles. The bottles were kept cold and dark in the field and frozen immediately upon return to the laboratory after sampling each day and remained frozen until analysis. We recognize that some DOM properties, such as fluorescence, may be influenced by the freezing process (Spencer et al., 2007); however, these changes are minimal for samples with relatively low DOC and $SUVA_{254}$, and we followed the recommendations of Fellman et al. (2010) for long term preservation.

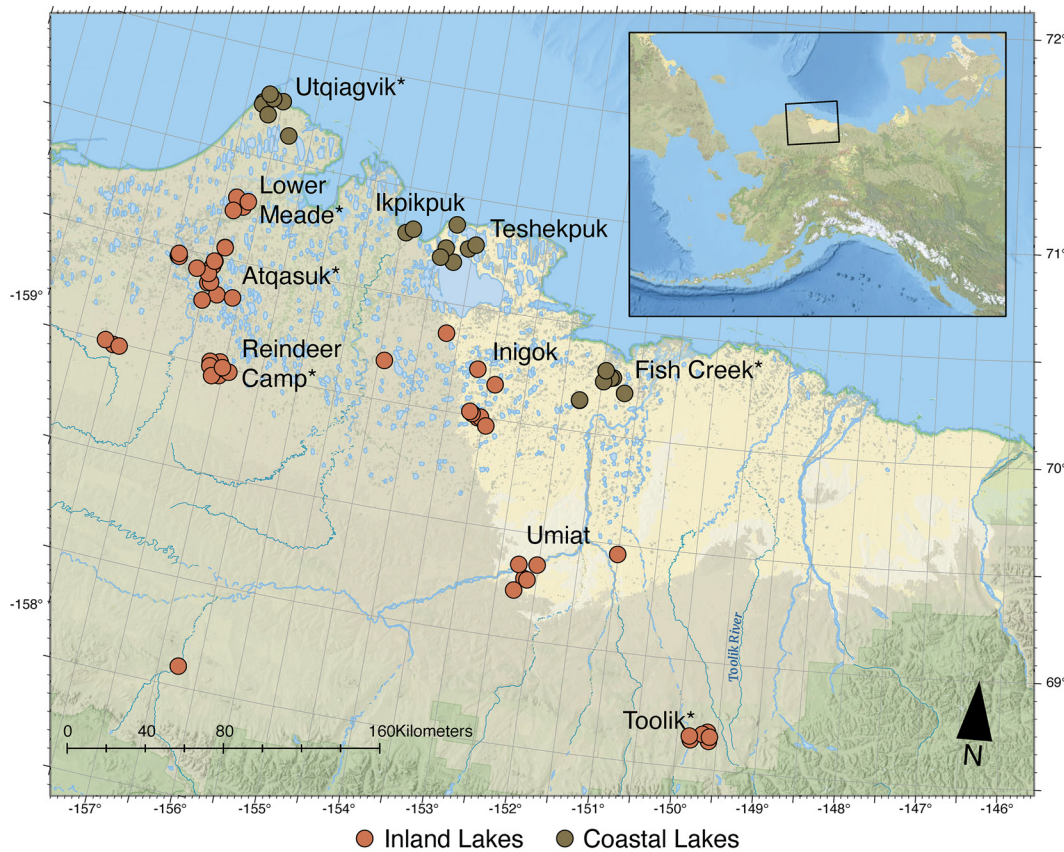

Figure 1. Map of the study site and sampling locations. Locations with an asterisk (*) indicate a lake from this region was analyzed using FT-ICR MS.

Meteorological data from 2012 to 2014 at each of the 10 lake regions were obtained from the Arctic Data Center repository (Hinkel, Lenters, Arp, et al., 2012) and include continuous monitoring of air pressure, solar radiation, air temperature, and relative humidity at a lake representing each region. For each lake, the median value was calculated across April (winter) and August (summer) every year and used for spatial analysis (Figures S1a—S1d in Supporting Information S1). Yearly lake ice thickness data from 2012 to 2014 were obtained from Arp (2018a) across surveyed lakes from regions in the North Slope.

2.2. DOC Concentration and Optical Analysis

Filtered water samples were acidified with HCl and analyzed for dissolved organic carbon concentration (DOC) on a Shimadzu TOC-L CPH high temperature catalytic oxidation total organic carbon analyzer (Shimadzu Corp., Kyoto, Japan). Samples were sparged with CO_2-free air to removed dissolved inorganic carbon prior to analysis and quantified using a 5-point calibration curve according to established methodology (e.g., Johnston et al., 2020; Kurek et al., 2020).

Absorbance spectra were measured in a 1-cm cuvette using a Horiba Scientific Aqualog (Horiba Ltd., Kyoto, Japan) at room temperature from wavelengths of 230–800 nm. Spectral slopes were calculated at 275–295 ($S_{275–295}$) and 350–400 nm ($S_{350–400}$), and the spectral slope ratio (S_R) was calculated by dividing $S_{275–295}$ by $S_{350–400}$ (Helms et al., 2008). Specific UV absorbance at 254 nm ($SUVA_{254}$; L mg C^{-1} m^{-1}) was calculated by dividing the decadic absorption coefficient at 254 nm by the DOC concentration in mg L^{-1} (Weishaar et al., 2003).

Excitation-Emission matrices (EEMs) were also measured in a 1-cm cuvette using a Horiba Scientific Aqualog (Horiba Ltd., Kyoto, Japan) at room temperature. EEMs were collected at excitation wavelengths of 250–500 nm and emission wavelengths of 300–600 nm with 5 and 2 nm intervals, respectively, with integration times between 1 and 10s. The EEMs were corrected for lamp intensity (Cory et al., 2010), inner filter effects (Kothawala

et al., 2013), and normalized to Raman units (Stedmon et al., 2003). Parallel factor analysis (PARAFAC) was conducted using 225 individual EEMs and validated using core consistency diagnostics and split-half validation using procedures described in Murphy et al. (2013), resulting in a 6-component model that explained 99.87% of the variance. The model was matched to previously identified components using an online library (www.openfluor.org; Murphy et al., 2013). Finally, the fluorescence index (FI) was calculated from the emission intensity at 470 and 520 nm at excitation 370 nm (Cory & McKnight, 2005; McKnight et al., 2001).

2.3. Solid Phase Extraction and FT-ICR MS

A subset (n = 40) of the samples was selected for FT-ICR MS analysis spanning both a longitudinal and latitudinal gradient. The samples were selected from eight individual lakes across six lake regions in each season between 2012 and 2014 (Figure 1, asterisks). Filtered water samples were acidified (pH 2), and solid phase were extracted using Bond-Elut PPL columns (Agilent Technologies Inc., Santa Clara, CA) following established procedures (Dittmar et al., 2008). PPL columns were prepared by soaking with methanol (>4 hr), rinsing once with methanol, and rinsing with Milli-Q water at pH 2 twice. 50 µg C was isolated onto 100 mg 3 mL bed volume PPL columns (assuming at least 65% recovery), eluted with 1 mL methanol into precombusted (550°C, >4 hr) glass vials, and stored at −20°C until analysis. Methanolic extracts were analyzed on a custom-built 9.4-T FT-ICR mass spectrometer (Oxford Corp., Oxney Mead, UK) with a 22 cm diameter bore at the National High Magnetic Field Laboratory (Tallahassee, FL; Blakney et al., 2011; Kaiser et al., 2011). Negatively charged ions from DOM were produced via electrospray ionization (ESI) at a flow rate of 500 nL min^{-1} and collected over 100 coadded scans. Peaks were internally calibrated based on highly abundant O-containing series as described previously (e.g., Kurek et al., 2020). Reproducibility of ultrahigh resolution mass spectrometry across multiple different instruments was previously reported by Hawkes et al. (2020), and reproducibility of this instrument was assessed by Zherebker et al. (2020).

Signals >6σ RMS baseline noise were exported to a peak list and processed using PetroOrg © (Corilo, 2014). Molecular formulae were assigned to ions constrained by $C_{4–45}H_{4–92}O_{1–25}N_{0–4}S_{0–2}$, and the mass measurement accuracy did not exceed 200 ppb error, similar to DOM measured in other high-latitude studies (e.g., Johnston et al., 2020; Kellerman et al., 2020). Additionally, molecular formulae assignment was constrained by stoichiometric ratios ($0.2 < H/C < 2.5$, $0 < O/C < 1$) described in Kind and Fiehn (2007). Molecular properties including the modified aromaticity index (AI_{mod}) were calculated according to Koch and Dittmar (2006; 2016) and the average carbon oxidation state (C_{OX}) after Mann et al. (2015). For each formula, stoichiometric ratios were calculated (H/C, O/C, N/C, S/C) as the sum of all heteroatoms divided by the sum of all carbon atoms and number-averaged across samples. Formulae were also grouped based on the percent relative abundance of their heteroatomic compositions as CHO, CHON, CHOS, and CHONS.

2.4. Statistical Analysis

PARAFAC modeling, calculation of optical indices, and generation of EEM spectra were conducted using Matlab with the drEEM toolbox (Murphy et al., 2013). Data analysis and visualization was done in R (R Core Team, 2020) using the ggplot2 package (Wickham, 2016). Linear regressions and hypothesis testing were also done using base R with comparisons of lake DOM properties between different years and seasons conducted using the nonparametric Kruskal–Wallis test at the $\alpha = 0.05$ significance level. Averages are reported as medians unless otherwise stated due to the non-normality of many of the variables. A Principal Component Analysis (PCA) of the lakes according to their DOM properties was done using the factoextra package in R (Kassambara & Mundt, 2017).

3. Results

3.1. Physical and Geochemical Properties of Tundra Lakes

Measured lake depths at the sampling spots ranged from 0.4 to 18.4 m but were mostly shallow with an average depth of 2.3 m and an inter-quartile range from 1.6 to 3.6 m. Air pressure and solar radiation were higher in the winter while air temperature and relative humidity were higher in the summer samples, with both air pressure and relative humidity increasing northward (Figures S1a–S1d in Supporting Information S1). Ice thickness (mean

Table 1
Median and Inter-Quartile Range (Q1–Q3) of Specific Conductivity (SpC), Water Temperature, Dissolved Oxygen (DO), and Chlorophyll-a Concentrations of Lakes From the Study Area in Summer and Winter

	Summer	Winter
Specific conductivity (SpC, μS cm^{-1})	152; 81–243 (n = 170)	304; 165–593 (n = 108)
Water temperature (°C)	10.4; 7.9–13.4 (n = 170)	0.8; 0.2–1.6 (n = 62)
Dissolved oxygen (DO, % saturation)	102.0; 99.0–107.0 (n = 118)	47.5; 17.8–80.5 (n = 62)
Chlorophyll-a (µg L^{-1})	1.5; 1.0–2.8 (n = 181)	1.3; 0.7–2.6 (n = 100)

Note. The number of measurements (n) are in parentheses.

and maximum thickness) varied in each region from 2012 to 2014 but generally increased going north and plateaued at the coastal sites including Ikpikpuk, Teshekput, and Utqiagvik (Figures S1e and S1f in Supporting Information S1).

Water temperatures were on average higher in the summer than in winter (10.4 vs. 0.8°C, respectively, $p < 0.001$) as well as DO (102.0 vs. 47.5%, respectively, $p < 0.001$). In contrast, SpC was on average higher in the winter than the summer (304 vs. 152 µS cm^{-1}, respectively, $p < 0.001$) often in a similar range to values measured from lakes and streams in western Greenland (e.g., Kellerman et al., 2020) but with high variance across the sites (Table 1). Chlorophyll-a concentrations were relatively low and in the same range as other oligotrophic arctic lakes (e.g., Breton et al., 2009) with no significant difference between seasons (average summer = 1.5 µg L^{-1}, winter = 1.3 µg L^{-1}, $p = 0.18$).

3.2. Tundra Lake DOC Concentration and DOM Optical Properties

Across the tundra lakes, the DOC concentration was significantly higher in the winter than summer (mean = 13.36 vs. 6.16 mg L^{-1}, respectively, $p < 0.001$) in all years and consistently higher each winter relative to the following summer (Figure 2a). Chromophoric dissolved organic matter absorbance measured at 254 nm (CDOM, a_{254}) was also significantly higher in the winter than the summer (mean = 58.85 vs. 20.73 m^{-1}, respectively, $p < 0.001$)

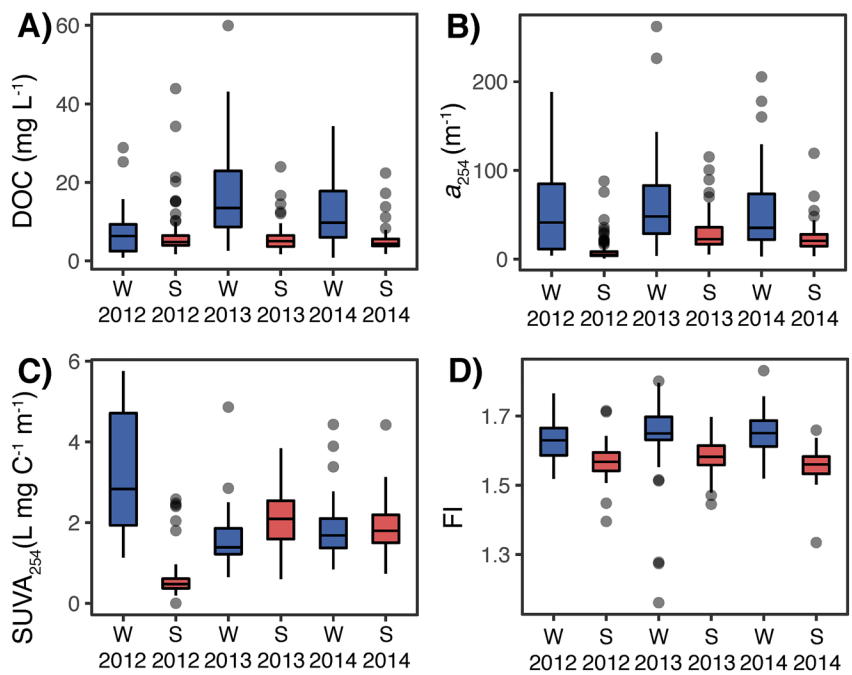

Figure 2. Boxplots of (a) DOC, (b) CDOM (a_{254}), (c) SUVA$_{254}$, and (d) FI of lakes from the study area from 2012 to 2014. Winter (W) samples are indicated by blue shading while summer (S) samples are shaded in red.

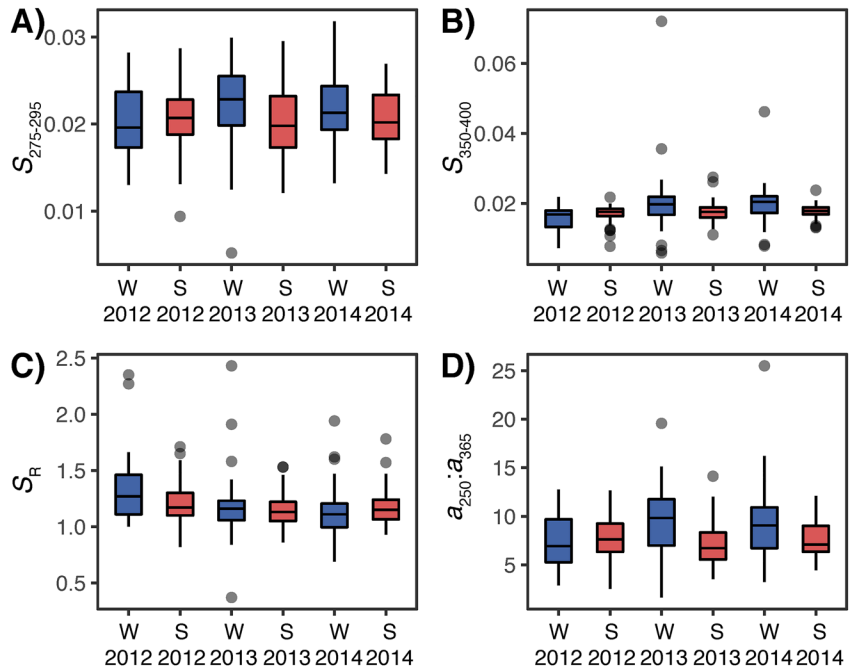

Figure 3. Boxplots of (a) $S_{275–295}$, (b) $S_{350–400}$, (c) S_R, and (d) a_{250}:a_{265} for lakes in this study area from 2012 to 2014. Winter (W) samples are indicated by blue shading while summer (S) samples are shaded in red.

as well as $SUVA_{254}$ (mean = 2.03 vs. 1.46 L mg C $^{-1}$ m^{-1}, respectively, $p < 0.001$; Figures 2b and 2c). CDOM was also higher each winter relative to the following summer (Figure 2b), whereas $SUVA_{254}$ was only higher in winter 2012 than the summer and lower in the following years (Figure 2c). Optical properties and DOC concentrations were in ranges consistent with previous measurements made across other high-latitude lakes; however, the DOC concentrations measured here were noticeably lower than in the Yukon Flats (Bogard et al., 2019; Johnston et al., 2020; Osburn et al., 2017; Shatilla & Carey, 2019; Stubbins et al., 2014). The fluorescence index (FI) followed similar seasonal trends where it was significantly higher in the winter than summer (mean = 1.64 vs. 1.57, respectively, $p < 0.001$) and also higher each winter relative to the following summer (Figure 2d). FI values across these sites were on average higher than in similar arctic lakes (Breton et al., 2009; Cory et al., 2007) but similar to arctic headwaters during low discharge and from permafrost-fed streams (Shatilla & Carey, 2019; Wickland et al., 2012; Wologo et al., 2021).

Other optical features including the spectral slope from 275 to 295 nm ($S_{275-295}$), the spectral slope from 350 to 400 nm ($S_{350-400}$), and the ratio between the absorbance at 250 and 365 nm (a_{250}:a_{365}) were all significantly higher in the winter than the summer ($p < 0.05$, 0.001, 0.001, respectively) and in all years except for 2012 where there was no difference between winter and summer (Figures 3a, 3b, and 3d). In contrast, the ratio of $S_{275-295}$ to $S_{350-400}$ (S_R) did not differ between winter and summer (Figure 3c). Spectral slopes and S_R were in similar ranges to other arctic lakes (Johnston et al., 2020; Osburn et al., 2017), but steeper than in major arctic rivers and permafrost soil porewaters (Frey et al., 2016; Mann et al., 2016).

DOC concentration and DOM composition also varied spatially across the Alaskan tundra (Figures S2 and S3 in Supporting Information S1), including with local meteorology. In the summer, CDOM absorbance and $SUVA_{254}$ correlated positively with solar radiation and relative humidity, and negatively with air temperature, while spectral properties including $S_{275-295}$ and a_{250}:a_{365} correlated negatively with relative humidity (Table S1). In contrast, there were no significant correlations with most winter DOM properties and local meteorology except for $S_{275–295}$ and a_{250}:a_{365} which correlated positively with lake ice thickness (Table S1). We also found no significant linear relationships with latitude except for $S_{275–295}$, $S_{350–400}$, and a_{250}:a_{365} which correlated negatively in the summer (Figure S3 in Supporting Information S1; Table S1), particularly in the western transect but not in the east (Table S2).

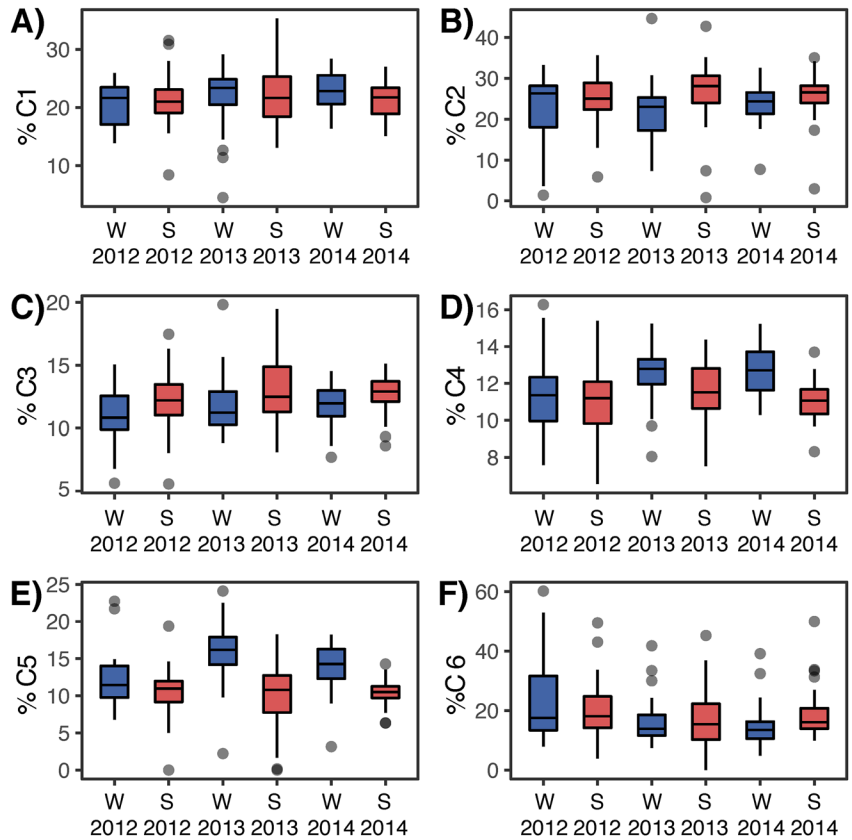

Figure 4. Boxplots of the percent fluorescence components (C1–C6) in lakes from this study area from 2012 to 2014. Winter (W) samples are indicated by blue shading while summer (S) samples are shaded in red.

3.3. PARAFAC modeling (FDOM composition)

PARAFAC analysis of the EEM spectra resulted in a six-component model (Figure S4 in Supporting Information S1) that was validated using split-half analysis (Figure S5 in Supporting Information S1). All six components (C1–C6) were compared with previously identified DOM fluorophores using the online library OpenFluor (Murphy et al., 2013). C1 (Ex_{330}, Em_{435}) was similar to peak C fluorophores (Coble, 1996) as well as terrestrial humic-like material (Groeneveld et al., 2020; Peleato et al., 2017). C2 (Ex_{265}, Em_{423}) was similar to peak A fluorophores (Coble, 1996) and also consistent with previously characterized terrestrial humic-like material (Lapierre & Del Giorgio, 2014; Peleato et al., 2017). C3 (Ex_{270}, Em_{518}) had a more red-shifted emission maximum than C2 and was similar to low apparent molecular weight terrestrial DOM components (Lambert et al., 2016; Wünsch et al., 2017). C4 ($Ex_{265,380}$, Em_{460}) was also consistent with allochthonous DOM, representing DOM from soils and microbially-derived humic-like components (Stedmon et al., 2011; Yamashita et al., 2011). C5 (Ex_{310}, Em_{377}) was similar to peak M fluorophores (Coble, 1996) likely derived from microbially processed aquatic DOM (Groeneveld et al., 2020; Lambert et al., 2016). C6 (Ex_{275}, Em_{327}) was similar to peak T fluorophores (Coble, 1996) and consistent with autochthonous protein-like tryptophan components (Lambert et al., 2016; Zhou et al., 2019).

3.4. FDOM Composition of Tundra Lakes

Fluorescent dissolved organic matter (FDOM) in the tundra lakes was significantly higher across all the winter samples than in the summer ($p < 0.001$) as well as within each year. Fluorescent components also differed in their percent composition between seasons (Figure 4). Winter FDOM was higher in percent C1 ($p < 0.001$), C4 ($p < 0.001$), and C5 ($p < 0.001$) than summer FDOM with C4 (mean winter = 12.4%, summer = 11.2%) and C5 (winter = 14.4%, summer = 10.5%) having the greatest relative differences (Figure 4). In contrast, summer FDOM was relatively enriched in C2 ($p < 0.001$), C3 ($p < 0.001$), and C6 ($p < 0.05$) compared to winter with C2 (winter = 22.7%, summer = 25.8%) and C3 (mean winter = 11.6%, summer = 12.6%) having the greatest

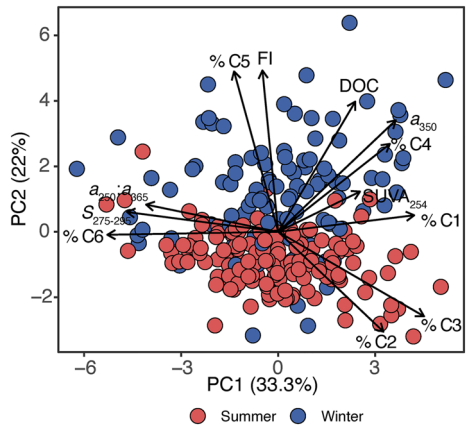

Figure 5. Principal component analysis (PCA) biplot of DOC concentrations and DOM properties of lakes from this study area from 2012 to 2014. Winter samples are indicated by blue shading while summer samples are shaded in red.

relative differences (Figure 4). We did not find significant linear relationships between FDOM and air pressure, solar radiation, air temperature, relative humidity, and latitude in either season except for winter ice thickness where %C2 correlated negatively and %C5 correlated positively (Table S1).

3.5. Drivers of optical and fluorescent DOM composition

DOC, optical indices, and fluorescent properties were ordinated into a PCA to visualize the main drivers in DOM composition across latitude and seasons (Figure 5). Over 55% of the total variance was explained by the first two principal components, with component 1 (PC1) explaining 33.3% and component 2 explaining an additional 22.0% (Figure 5). PC1 was strongly influenced by %C6, $S_{275–295}$, %C3, %C1, and a_{250}:a_{365}, whereas PC2 was driven by FI, %C5, DOC, a_{350}, and %C2. Lakes were separated by season along PC2 with winter samples (blue points) scattered predominantly above zero and summer samples (red points) predominantly below zero, whereas samples from both seasons was spread along PC1 (Figure 5). Additionally, we found no trends between either principal component with sampling sites, lake regions, transects, or sediment types (Figure S6 in Supporting Information S1).

The principal component loadings of each sample were compared to several physical, geochemical, and morphological variables including, DO, water temperature, SpC, chlorophyll-*a*, lake depth, lake area, elevation, and latitude (Table S3). PC1 correlated negatively with lake depth ($r^2 = 0.12$, $p < 0.001$; Figure 6a), lake area ($r^2 = 0.05$, $p < 0.01$), and the product of lake depth and lake area representing an estimation of lake volume ($r^2 = 0.16$, $p < 0.001$) but did not correlate significantly with the other variables (Table S3). PC2 correlated negatively with DO ($r^2 = 0.37$, $p < 0.001$) and water temperature ($r^2 = 0.25$, $p < 0.001$ (Figures 6b and 6c), and positively with SpC ($r^2 = 0.18$, $p < 0.001$). Finally, neither component correlated significantly with latitude.

3.6. FT-ICR MS DOM Composition of Tundra Lakes

A subset of the lakes was analyzed using FT-ICR MS in both seasons to characterize their DOM molecular composition (Table S4). DOM stoichiometries were similar to other high-latitude lakes (Johnston et al., 2020; Kellerman et al., 2020) and were similar in saturation but more oxygenated than several arctic permafrost-fed streams (Wologo et al., 2021). Furthermore, DOM was more similar within individual lakes than within seasons. To illustrate, we identified 480 shared molecular formulae common across all summer samples representing 17%–33% of the total relative abundance of each. Similarly, we found 951 common molecular formulae across all winter samples representing 31%–39% of the total relative abundance of each. In contrast, there were more common formulae within each lake representing 1,840-4,187 molecular formulae that accounted for the majority of the relative abundance in each sample (Table S5).

There were more significant correlations between FT-ICR MS DOM properties and local meteorology in the summer samples than in the winter (Table S6). Properties describing aromaticity and aliphaticity (H/C, AI_{mod}, C_{OX}) correlated significantly with solar radiation in the summer, similar to CDOM and $SUVA_{254}$ (Table S1), but not in the winter (Table S6). However, most significantly correlated FT-ICR MS DOM properties included heteroatom content such as %CHON, %CHOS, and %CHO in both seasons (Table S6). To illustrate, %CHO decreased with air pressure and relative humidity and increased with solar radiation and air temperature (Figure 7), with the inverse occurring for %CHON, %CHOS, N/C, and S/C (Table S6 in Supporting Information S1). In both the summer and the winter, heteroatom content and latitude also correlated significantly with the percent relative abundance of heteroatoms increasing with latitude and %CHO decreasing (Table S6 in Supporting Information S1).

The molecular formulae that were common within summer and winter samples and those unique to only summer and only winter were identified and compared across the lakes to understand how molecular properties differed between seasons. This analysis included all samples except those from the lake in Atqasuk because it had the least number of common formulae between each season representing the lowest relative abundance (Table S5). DOM from Atqasuk also had much higher H/C ratios and lower O/C ratios and AI_{mod} values than any other DOM

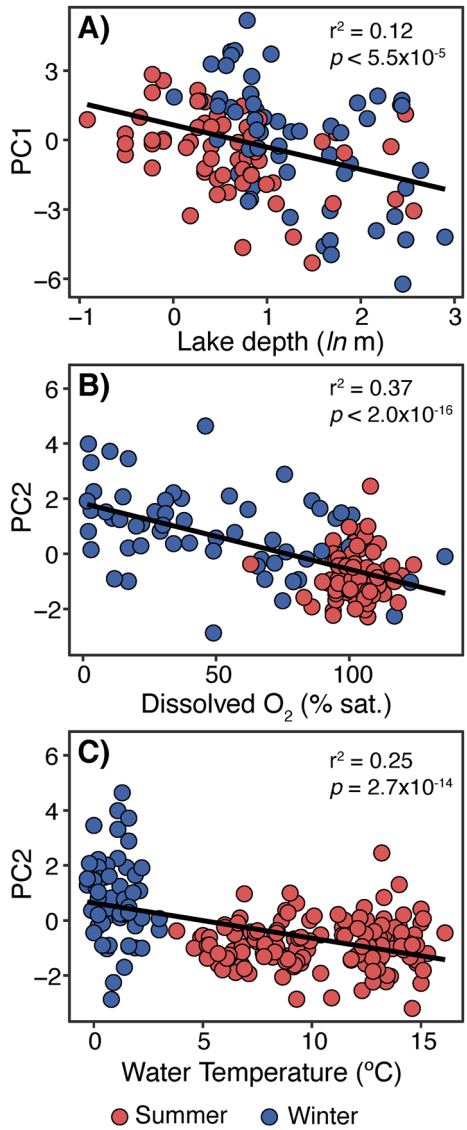

Figure 6. Linear regressions of (a) PC1 versus. log-transformed Lake depth, (b) PC2 versus. dissolved oxygen, and (c) PC2 versus water temperature for lakes from the PCA in Figure 5. Winter samples are indicated by blue shading while summer samples are shaded in red.

sample in the dataset (Table S4) in addition to consistently lower SpC (Hinkel et al., 2017), suggesting that the lake had significantly different geochemical properties and DOM processing from the other lakes.

We first identified and compared the molecular formulae present in all of the summer (1,024) and winter (1,363) samples (Figures 8a and 8b). DOM formulae common across the summer samples had significantly higher molecular weight, O/C, and AI_{mod} than common winter formulae and lower H/C and C_{OX} (Table S7), though there was great variability between molecular formulae in van Krevelen space. This can be seen as the distribution of points in Figure 8b is shifted slightly higher than in Figure 8a, suggested greater aliphaticity. We next identified the formulae that were strictly unique to just summer samples and winter samples and removed those that were shared between both seasons (Figures 8c and 8d). This approach is advantageous because by isolating the formulae that are unique to each season, we compared how they differed in composition individually without the effects of the shared formulae. Similarly, formulae unique to summer had significantly higher average molecular weight, O/C, and AI_{mod} than winter formulae and lower H/C and C_{OX} (Table S7) with both groups displaying high variability in van Krevelen space. The same trend can be seen as the point distribution in Figure 8d is shifted to the top left corner (compare Figure 8c). Additionally, there were almost twice as many unique winter formulae than in the summer (Table S7) with a greater distribution of CHON and CHOS formulae (Figures 8c and 8d).

4. Discussion

4.1. Spatial Patterns of Tundra DOM Composition

DOM composition in the Alaskan tundra varied across lakes and displayed few consistent trends with latitude from Toolik to Utqiagvik (Figures 1 and S2 in Supporting Information S1). Furthermore, while CH_4 concentrations from lakes in this region have correlated with latitude, there were no significant relationships between latitude and DOC (Townsend-Small et al., 2017), suggesting that organic matter and DOM composition across these lakes are heterogeneous and governed by local physical and biogeochemical processes. These findings were not entirely unexpected given that the samples also encompassed different sediment types (Elder et al., 2018; Hinkel et al., 2005), geochemical properties (Hinkel et al., 2017, Table 1), and diverse local meteorological conditions (Figure S1 in Supporting Information S1). Here, we focus on the latter and discuss how some of the spatial patterns of DOM properties are influenced by local conditions that covary with latitude (Zhang et al., 1996; Hinkel, Lin, et al., 2012; Figure S1 in Supporting Information S1).

Across both transects, the local meteorology illustrated differences between the northern coastal (Utqiagvik, Ikpikpuk, Teshekput, Fish Creek) and inland lakes (Figure 1). Coastal lakes generally had higher air pressure, relative humidity, and winter ice thickness than the inland lakes (Figures S1a, S1d–S1f in Supporting Information S1). However, other relationships were more complex, such as temperature which was slightly higher on the coast during the winter and slightly lower in the summer (Figure S1c in Supporting Information S1; Zhang et al., 1996; Hinkel, Lin, et al., 2012), and incoming solar radiation (Figure S1b in Supporting Information S1), which is influenced by many physical features (Dymond & Johnson, 2002). Differences between coastal and inland lakes could also be seen in bulk- and molecular-level DOM properties. DOM properties describing aromaticity such as CDOM absorbance and $SUVA_{254}$ correlated positively with relative humidity while spectral slope parameters (a_{250}:a_{365}, $S_{275\text{-}295}$) correlated negatively with relative humidity (Table S1), suggesting DOM from lakes closer to the coast were more aromatic and of greater molecular weight (Helms et al., 2008; Weishaar

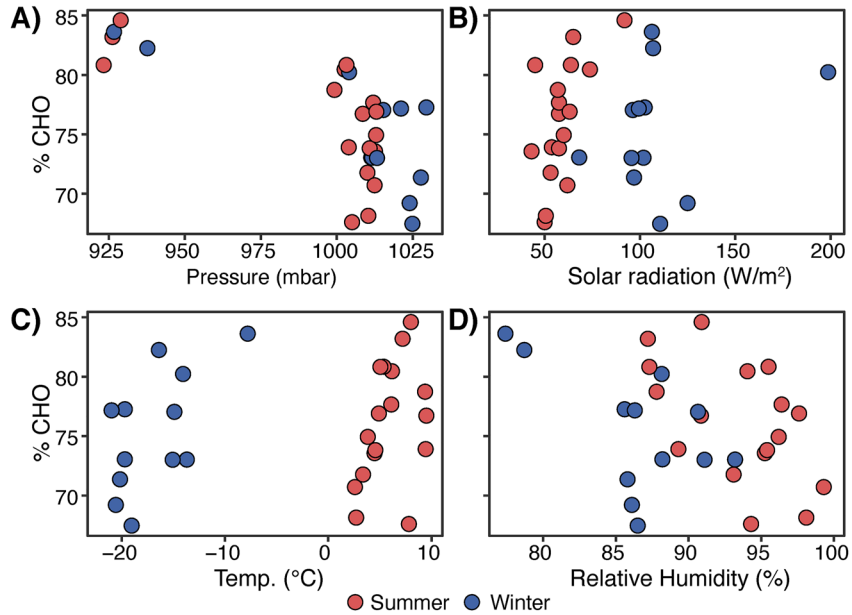

Figure 7. Scatterplots of the percent relative abundance of CHO-containing formulae with (a) air pressure, (b) solar radiation, (c) air temperature, and (d) relative humidity of lakes from this study area from 2012 to 2014. Winter samples are indicated by blue shading while summer samples are shaded in red.

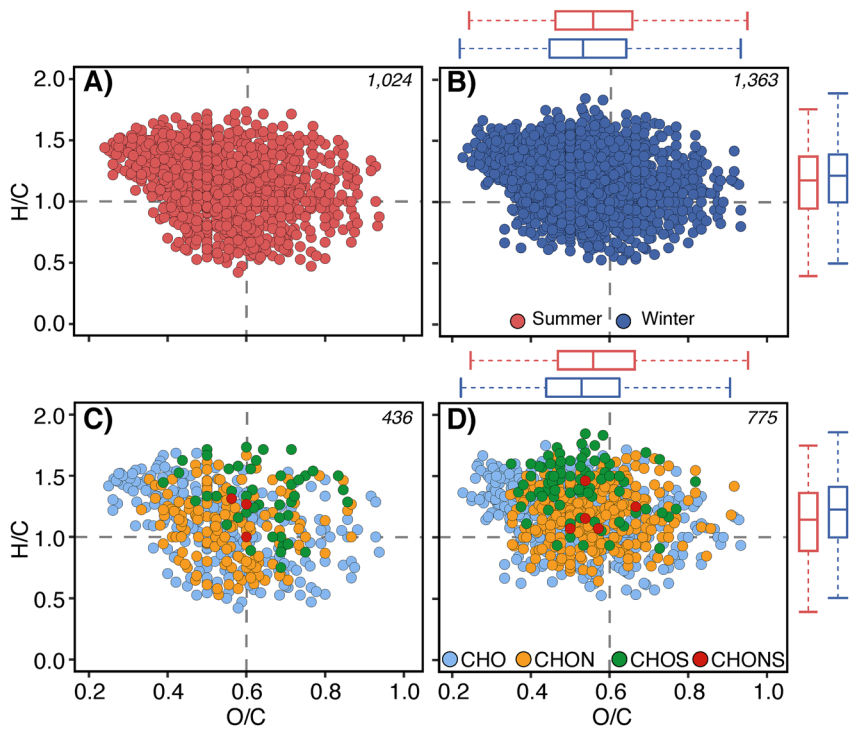

Figure 8. van Krevelen diagrams of molecular formulae (a) common in all summer samples (1,024), (b) common in all winter samples (1,363), (c) unique to only summer samples (436), and (d) unique to only winter samples (775). Molecular formulae include all samples except those from Atqasuk. Box plots on the *x*-axis represent the O/C ratios, while box plots on the *y*-axis represent the H/C ratios. Box plots associated with panels A and B represent the common summer and winter formulae and box plots associated with panels C and D represent the unique formulae. Colors in panels A and B represent summer (red) and winter (dark blue), while in panels C and D represent CHO (light blue), CHON (orange), CHOS (green), and CHONS (red) containing formulae.

et al., 2003). Higher aromaticity in the coastal lake DOM is also supported by the negative correlations of CDOM absorbance and $SUVA_{254}$ with summer air temperature (Table S1) since coastal lakes tend to have lower summer air temperature than inland lakes (Figure S1c in Supporting Information S1). Other molecular level properties such a heteroatom content (%CHON, %CHONS) also correlated positively with relative humidity and air temperature while %CHO decreased (Figure 7; Table S6), indicating that N- and S-containing DOM compounds were more abundant in coastal lakes than inland lakes (Table S6).

Coastal tundra lakes are susceptible to storm surges, high wind, and erosion resulting in ecological changes to vegetation and lakeshores (Arp et al., 2010). Many of these effects, including precipitation, temperature, and vegetation, have been shown to influence DOM composition and processing across similar arctic lakes (Johnston et al., 2019; Kellerman et al., 2020), and are likely contributing to the spatial differences between aromaticity and spectral slopes across this region. In addition, the high N- and S-content of coastal lakes may reflect some marine influence on lake DOM via aerosolization as marine DOM compounds are often more heteroatomic-rich than freshwater DOM (D'Andrilli et al., 2015; Kellerman et al., 2018; Kurek et al., 2020). The resulting aerosols are enriched in N- and S-containing compounds from marine DOM (Rastelli et al., 2017; Schmitt-Kopplin et al., 2012), that can be transferred to coastal lakes during storms and incorporated into the bulk DOM.

Although latitude was generally a poor predictor for DOM composition, some spectral indices including $S_{275–295}$, $S_{350–400}$, and a_{250}:a_{365}, did correlate weakly with latitude (Table S1), but were restricted to the western transect above 70.5° N (Figure S3 in Supporting Information S1; Table S2). Rather than being a latitudinal trend, this correlation was most likely due to the northernmost lakes at Utqiagvik having shallower spectral slopes than the other regions (Figure S3) and is probably related to differences in DOM sourcing since lakes from this region have greater CO_2 and CH_4 emissions that are also older (Elder et al., 2018). In contrast, the negative correlation between %CHO-containing formulae and latitude was much stronger and not necessarily nested in the northernmost site (Table S6). Instead, this trend could also reflect differences in DOM sources as different permafrost and soil types leach compositionally different DOM (MacDonald et al., 2021), or proximity to fluvial sources (Figure 1) since decreased hydrologic connectivity can increase the amount of N- and S-containing DOM compounds in arctic lakes (Johnston et al., 2020). These trends were also observed across only eight individual lakes, meaning FT-ICR MS analysis of additional lakes from the pan-Arctic may help further constrain their spatial relationships with DOM and this facet is currently being investigated in a separate study. Additionally, while some relationships with DOM and local conditions were statistically significant, many were relatively weak (Tables S1 and S6), possibly owing to upscaling of regional meteorology from single lakes, and future work should be focused on greater spatial resolution of physical and meteorological data to further assess their relationships to lake DOM.

4.2. The Importance of Seasonality in Tundra DOM Cycling

In contrast to the weak spatial patterns, DOC and DOM properties differed significantly between summer and winter (Figures 2–4). While we recognize that winter stratification concentrates solutes in the bottom water (Jansen et al., 2021), we maintain that our samples collected directly under the ice were representative of DOM in these lakes. Most lakes in this study were shallow between 1.6 and 3.6 m with thick ice cover ranging from 1.0 to 2.1 m (Figure S1 in Supporting Information S1), meaning that winter sampling did occur near the bottom in many lakes. Furthermore, peak stratification in this region has been shown to appear primarily the during ice-out period (Hinkel, Lenters, Sheng, et al., 2012; Townsend-Small et al., 2017), which occurred several weeks after our winter sampling.

DOM composition clearly separated lakes by season, accounting for up to 22% of the variance between samples (Figure 5) and was linked to changes in water temperature and DO (Figures 6b and 6c). These seasonal differences were less apparent in individual FT-CIR MS samples likely due to the small number of lakes sampled for FT-ICR MS analysis, the molecular selectivity of SPE-PPL (Perminova et al., 2014), and the preferential ionization of electrospray negative for carboxylic acids, thereby omitting many microbially derived molecular formulae (Kurek et al., 2020, 2021). However, when considering the bulk optical and fluorescent properties across all samples, DOM in the winter was generally higher in aromatic moieties (i.e., higher in a_{254}), of lower molecular weight (i.e., steeper spectral slope values), and with greater total fluorescence (i.e., higher FDOM) than summer (Figures 2–4), likely due to formation of thick lake ice and the under ice-processing that occurred throughout winter until sampling in April.

During ice formation, inorganic and organic solutes are excluded from the ice crystals and accumulate in the water column as the water volume is reduced (Belzile et al., 2002), resulting in higher DOC concentrations, CDOM, FDOM, and SpC in the winter than the summer (Table 1, Figures 2–4). Ice exclusion also impacted the inherent DOM molecular composition resulting in seasonal, and to some extent, annual variations. For instance, $SUVA_{254}$ was greater in winter 2012 than any other winter or summer (Figure 2c). However, this was due to the lower average DOC concentrations that year rather than absorbance (Figures 2a and 2b), suggesting that the proportion of DOC excluded from the ice was relatively more aromatic in 2012 than the following years (Figure S7 in Supporting Information S1). Similarly, the proportion of fluorescent components varied between seasons. DOM underneath the ice was consistently enriched in microbially processed FDOM from both allochthonous (C4) and autochthonous (C5) sources, which coincided with the high diversity of winter aliphatic and N,S-containing molecular formulae (Figures 4 and 8). This seasonal DOM fractionation and seemingly contradictory nature of molecular compositions (e.g., high CDOM and aliphatic DOM compounds) suggests that under ice conditions are a dynamic period for biogeochemical cycling (Denfeld et al., 2018; Hampton et al., 2015) and are the result of several interwoven physical and biological processes.

First, in many high-latitude lakes, winter is accompanied by a shift from net autotrophy to heterotrophy which influences both the quantity and quality of respired carbon (Ducharme-Riel et al., 2015; Vachon, Solomon, & del Giorgio, 2017; Bogard et al., 2019). Winter heterotrophy was indicated by a slightly greater average ratio of DOC:SpC in summer than in the winter (median = 0.038 vs. 0.031, respectively, $p = 0.057$). If evaporation and concentration effects via winter ice exclusion and dilution from rainfall/overland flow were the only factors influencing aquatic DOC, then there should be no seasonal differences in the ratios (Kellerman et al., 2020). Instead, greater DOC per unit of SpC in the summer suggests DOC accumulated in these lakes, likely from both primary production and terrestrial inputs during the freshet, while processing and respiration in winter removed DOC. However, the difference in ratios between the seasons is small and may reflect slower rates of aquatic respiration due to lower winter temperatures (Ducharme-Riel et al., 2015). In addition, the ratios varied across the sampling years, particularly during 2012 (median winter = 0.019, summer = 0.036) where there was also a different relationship between DOC and CDOM (Figure S7 in Supporting Information S1), indicating that DOM input to these tundra lakes is heterogeneous and long-term processing could be susceptible to external influences such as temperature and precipitation variability.

Under-ice heterotrophy is also supported by the presence of many unique aliphatic and N,S-containing DOM formulae in the winter (Figure 8d), increases in FI (Figure 2d), and steeper spectral slope parameters (Figure 3), all of which are associated with increased freshness and microbial processing (D'Andrilli et al., 2015; Lambert et al., 2016; Spencer et al., 2015; Valle et al., 2018). This processed DOM is likely relatively young and is respired during the winter leading to high CO_2 concentrations accumulating underneath the ice (Elder et al., 2018). Additionally, the increase in unique molecular formulae, molecular level aliphaticity, and decrease in aromaticity in winter DOM (Figure 8; Table S7) further support the presence of fresh, microbial DOM underneath the ice, even though the overall absorbance has increased but only due to concentration of solutes via ice exclusion (Figure 2b). Under-ice DOM processing was also indicated by fewer significantly correlated DOM properties with local conditions in the winter than summer (Tables S1 and S6), suggesting ice cover disconnected lake DOM from external processes. The exception to this being a_{250}:a_{365}, $S_{275–295}$, %C5, and %CHON correlating positively with lake ice in the winter while %C2 correlated negatively (Tables S1 and S6), suggesting that regions with thicker lake ice in the winter had greater proportions of processed autochthonous DOM.

Finally, photolysis has been shown to degrade CDOM and produce aliphatic compounds as well as DIC which can contribute to lake CO_2 emissions (Allesson et al., 2020; Cory et al., 2007; Koehler et al., 2014). Since winter lakes were sampled in April, they were likely covered by peak snow thickness ranging from 10 to 83 cm (Arp, 2018b) that attenuated and reflected much of the incoming radiation, as similar snowpack has been shown to only transmit less than 1% of photosynthetically active radiation into lakes (Ducharme-Riel et al., 2015). Thus, while CDOM absorbance was higher underneath the ice owing to ice exclusion and concentration of solutes (Figure 2b), we also expected the aromaticity to be greater from reduced photodegradation. In contrast, we found no significant difference between the average ratio of CDOM (a_{350}) normalized to SpC between the summer and winter (median summer = 0.117, winter = 0.115, respectively, $p = 0.87$).

The ratios of CDOM:SpC suggest that the aromatic DOM composition was similar between late summer and winter, and since terrestrial DOM input is limited during the winter, much of the aromaticity must have been

retained from DOM sampled in August. This also suggests that late summer photolysis in tundra lakes may not be as important for shaping water column DOM composition as it is during the ice-out period, when most of the photodegradation and terrestrial DOM transport occurs (Michaelson et al., 1998; Vachon et al., 2017). Consequently, photomineralization may only be a minor contributor to arctic CO_2 fluxes as many lakes experience increased browning (Allesson et al., 2020) and terrestrial DOM input likely outpaces photodegradation, even in lakes with long residence times (Cory et al., 2007). For instance, solar radiation in the summer correlated positively with bulk and molecular level aromaticity from both the optical and FT-ICR MS data (Tables S1 and S6), the opposite of what would be expected from photodegradation. Instead, the correlations may represent landscape processes like the relationship between solar radiation and terrestrial vegetation (Dymond & Johnson, 2002), where regions that experience more sunlight have greater plant biomass and input of aromatic compounds during summer mobilization events. Alternatively, the relationship may also describe warming-induced permafrost thaw where regions experiencing greater active layer degradation leach aromatic compounds from soil into the surrounding waters (MacDonald et al., 2021; Spencer et al., 2015). To fully understand the balance between terrestrial input, photodegradation, and the effects browning will have on tundra carbon cycling, sampling resolution must be expanded to capture the highly dynamic transition from ice cover through the ice-out period.

4.3. Potential Drivers of DOM Heterogeneity and Implications for a Changing Arctic

While seasonality explained PC2, it only represented 22.0% of the total variance in DOM across the lakes (Figure 5). Most of the variance (PC1, 33.3%) was still unaccounted for and poorly explained by geochemical and water quality variables. For instance, there were no significant correlations between PC1 and SpC or chlorophyll-*a* concentrations (Table S3), suggesting that neither hydrologic setting, via subsurface flow (Hinkel et al., 2017) and evaporation (Anderson & Stedmon, 2007), nor primary productivity suitably predicted the differences in DOM properties across the lakes. Furthermore, while some studies have suggested high efficiency in boreal lake carbon cycling from autochthonous production (Bogard et al., 2019; Johnston et al., 2020), DOM in other high-latitude lakes seem to be controlled by allochthonous input (Allesson et al., 2020; Osburn et al., 2017), highlighting the range and uncertainty in aquatic carbon cycling across different arctic regions. Indeed, in the Alaskan tundra a large portion of DOM in the lakes originated from terrestrial sources given their low productivity (Stackpoole et al., 2017), the correlation between DOC and CDOM (Figure S7 in Supporting Information S1), the weak relationship between DOC and chlorophyll-*a* ($r^2 = 0.07$, $p < 0.001$), and the high proportions of terrestrial fluorophores (C2 and C3) in the summer (Figures 4b and 4c).

In addition to sourcing, other factors including transport, processing, and geomorphology may also influence the DOM composition (Cory et al., 2007; Woods et al., 2011; Wang et al., 2018). Tundra lakes vary in their regional morphology due to differences in eroded sediment and lake bathymetry (Hinkel et al., 2005), thus we propose that geomorphology and residence time are important regulators for DOM composition in tundra lakes, as has been suggested across some boreal lakes (Kellerman et al., 2014). To illustrate, PC1 correlated negatively with lake depth and lake area suggesting a link between DOM and lake morphology (Table S3; Figure 6a). Although the r^2 was relatively small, its effects are likely underestimated due to fewer samples collected in 2014 and from the difficulty in defining the dynamic shorelines of these lakes across multiple years (Hinkel, Lin, et al., 2012). Furthermore, lake depth was only measured as the deepest point at the sampling sites, meaning there is likely variability in the "true" depth and that lake volume may be a more suitable predictor of DOM composition in subsequent studies. We estimated lake volume as the product of lake depth and lake area (lake depth *x* lake area) and found a stronger negative correlation with PC1 than either lake depth or lake area alone ($r^2 = 0.16$, $p < 0.001$; Table S3).

There was also a difference in response based on season, resulting in a stronger correlation when the relationships between lake depth and lake depth *x* lake area with PC1 were modeled as a multiple linear regression with season as an additive term (lake depth: $r^2 = 0.21$, $p < 0.001$; lake depth *x* lake area: $r^2 = 0.21$, $p < 0.001$). Given that there was no relationship between these variables and PC2 (Table S3), this suggests that rather than being a seasonal control of DOM, lake geomorphology influences the overall mechanisms behind DOM processing in a similar way between seasons (i.e., same slopes), but ice formation and under-ice dynamics influence the starting composition at each season (i.e., different intercepts), such as during winter 2012 (Figures 2–4). Therefore, geomorphology, including lake depth, area, and bathymetry, may be an overall regulator for DOM composition

and the extent of under-ice microbial processing, both of which have implications for greenhouse gas emissions as similar relationships have been demonstrated for lake depth and CO_2 fluxes (Ducharme-Riel et al., 2015).

Indeed, the DOM composition in deep arctic lakes may be highly influenced by fresh microbially produced DOM given that the greatest contributors to PC1 were from C6 fluorescence and $S_{275–295}$ (Figure 5), possibly originating from the sediment that was disconnected from surface processes. In deep lakes, water column stratification produces hypoxic conditions at the bottom and promotes the release of microbial DOM and CH_4 from sediments (Gonsior et al., 2013; Townsend-Small et al., 2017; Valle et al., 2018). Given that some of the lakes from the study were deep (>3.6 m), DOC and DOM may have accumulated in the bottom water that was not captured in our under-ice sampling, resulting in an underestimation of DOC and CDOM absorbance for those lakes. This underestimation could partially explain the deviation of deep lakes from the regression line in Figure 6a, particularly for the winter samples, and influence the ratios of DOC and CDOM to SpC which would affect seasonal production or removal (Jansen et al., 2021). Furthermore, DOM from deep stratified lakes may have greater compositional differences that were not detected, such as in protein-like fluorescence and spectral slopes, which contributed to PC1 (Figure 5). However, much of the variance between PC1 and lake depth was still unexplained meaning it was most likely impacted by other processes such as hydrologic connectivity (Johnston et al., 2020), active layer detachments (Wang et al., 2018; Woods et al., 2011), or thermokarst coverage (Olefeldt et al., 2016). Delineating these processes and characterizing the DOM composition throughout the water column in stratified lakes will be important for constraining the extent of arctic carbon cycling and upscaling local differences to the regional level.

As the Arctic continues to warm, it will experience landscape changes that will inevitably impact the aquatic carbon cycle (Anderson et al., 2017). The tundra has been experiencing some of the greatest warming throughout Alaska and the Arctic (Wendler et al., 2017), making it particularly sensitive to disruptions in carbon cycling. Changes in local weather such as air temperature, pressure, humidity, solar radiation (Tables S1 and S6; Figure 7) as well as precipitation and snowfall will likely influence the overall seasonal DOM composition. For instance, warmer snowier winters have reduced ice growth across tundra lakes, shifting many lakes from bedfast to floating ice (Arp et al., 2012, 2015). This shift will degrade surrounding permafrost (Arp et al., 2016), and delay ice-out on lakes that now experience floating ice conditions, as well as expand overwintering fish habitat and winter water supply (Arp et al., 2015). Expansion of water under frozen lakes will provide microorganisms with greater access to DOM for consumption and respiration, for the duration of winter, amplifying winter carbon cycling in lakes that were once inactive for most of the year.

Additionally, we hypothesize an increase in winter DOM processing, and subsequently heterotrophy, in lakes that shift to floating ice from greater nutrient and substrate availability through the mobilization of additional permafrost sources via thermokarst expansion and active layer detachment (Abbott et al., 2015; Jones et al., 2011). Ice thinning and reduced snowpack will also reduce the physical barrier protecting DOM from UV radiation under ice, potentially inducing photomineralization of aromatic DOM after snowmelt. Ultimately, increased winter heterotrophy and photolysis will likely result in greater buildup of greenhouse gases under ice and subsequent emission after ice-out in large bursts, highlighting the importance of this short period to annual carbon emissions (Ducharme-Riel et al., 2015; Phelps et al., 1998; Vachon et al., 2017). Therefore, future efforts should focus on tracking the DOM composition and concentrations of dissolved greenhouse gases in succession through late winter and ice-out, as well the photo- and biolability potential of DOM as lakes transition from winter heterotrophy to summer phototrophy. Sampling locations in future studies will also become more important as warming and ice-out will likely have a disproportionate impact on lakes closer to the coast, which on average have more bedfast ice and could compound with nearby maritime effects including warming of the Arctic Ocean and marine aerosols. As we have demonstrated in this study, these combined effects will likely influence how DOM is cycled across arctic lakes seasonally and potentially on interannual timescales as carbon is transferred from aquatic interfaces to the atmosphere.

Conflict of Interest

The authors declare no conflicts of interest relevant to this study.

Data Availability Statement

The authors declare that all data supporting the results of this study are archived in the Earth Chem Library (https://doi.org/10.26022/IEDA/112233).

Acknowledgments
This work was conducted thanks to funding from the NSF Arctic Observing Network (AON): AON-1107596 to K. E. F., AON-1107607 to A. T. S., and AON-1107481 to C. D. A. Part of this work was performed at the National High Magnetic Field Laboratory ICR User Facility, which is supported by the National Science Foundation Division of Chemistry through DMR-1644779 and the State of Florida. We thank Ben Gaglioti and Ned Rozell for assistance with winter field sampling, Jim Webster and Louis Farquharson for assistance with summer field sampling, and Ben Jones and Guido Grosse in both seasons.

References

Abbott, B. W., Jones, J. B., Godsey, S. E., Larouche, J. R., & Bowden, W. B. (2015). Patterns and persistence of hydrologic carbon and nutrient export from collapsing upland permafrost. *Biogeosciences*, *12*(12), 3725–3740. https://doi.org/10.5194/bg-12-3725-2015

Allesson, L., Koehler, B., Thrane, J. E., Andersen, T., & Hessen, D. O. (2020). The role of photomineralization for CO2 emissions in boreal lakes along a gradient of dissolved organic matter. *Limnology & Oceanography*, *66*(1), 158–170. https://doi.org/10.1002/lno.11594

Anderson, N. J., Saros, J. E., Bullard, J. E., Cahoon, S. M., McGowan, S., Bagshaw, E. A., & Yde, J. C. (2017). The Arctic in the twenty-first century: Changing biogeochemical linkages across a paraglacial landscape of Greenland. *BioScience*, *67*(2), 118–133. https://doi.org/10.1093/biosci/biw158

Anderson, N. J., & Stedmon, C. A. (2007). The effect of evapoconcentration on dissolved organic carbon concentration and quality in lakes of SW Greenland. *Freshwater Biology*, *52*(2), 280–289. https://doi.org/10.1111/j1365-2427.2006.01688.x

Arp, C. D. (2018b). *Arctic Alaska tundra and lake snow surveys from 2012-2018*. Arctic Data Center. https://doi.org/10.18739/A2086356K

Arp, C. D. (2018a). *Lake ice thickness observations for arctic Alaska from 1962 to 2017 Arctic Data Center*. https://doi.org/10.18739/A2VM42X50

Arp, C. D., Jones, B. M., Grosse, G., Bondurant, A. C., Romanovsky, V. E., Hinkel, K. M., & Parsekian, A. D. (2016). Threshold sensitivity of shallow Arctic lakes and sublake permafrost to changing winter climate. *Geophysical Research Letters*, *43*(12), 6358–6365. https://doi.org/10.1002/2016gl068506

Arp, C. D., Jones, B. M., Liljedahl, A. K., Hinkel, K. M., & Welker, J. A. (2015). Depth, ice thickness, and ice-out timing cause divergent hydrologic responses among Arctic lakes. *Water Resources Research*, *51*(12), 9379–9401. https://doi.org/10.1002/2015wr017362

Arp, C. D., Jones, B. M., Lu, Z., & Whitman, M. S. (2012). Shifting balance of thermokarst lake ice regimes across the Arctic Coastal Plain of northern Alaska. *Geophysical Research Letters*, *39*(16). https://doi.org/10.1029/2012gl052518

Arp, C. D., Jones, B. M., Schmutz, J. A., Urban, F. E., & Jorgenson, M. T. (2010). Two mechanisms of aquatic and terrestrial habitat change along an Alaskan Arctic coastline. *Polar Biology*, *33*(12), 1629–1640. https://doi.org/10.1007/s00300-010-0800-5

Battin, T. J., Luyssaert, S., Kaplan, L. A., Aufdenkampe, A. K., Richter, A., & Tranvik, L. J. (2009). The boundless carbon cycle. *Nature Geoscience*, *2*(9), 598–600. https://doi.org/10.1038/ngeo618

Belzile, C., Gibson, J. A., & Vincent, W. F. (2002). Colored dissolved organic matter and dissolved organic carbon exclusion from lake ice: Implications for irradiance transmission and carbon cycling. *Limnology & Oceanography*, *47*(5), 1283–1293. https://doi.org/10.4319/lo.2002.47.5.1283

Blakney, G. T., Hendrickson, C. L., & Marshall, A. G. (2011). Predator data station: A fast data acquisition system for advanced FT-ICR MS experiments. *International Journal of Mass Spectrometry*, *306*(2–3), 246–252. https://doi.org/10.1016/j.ijms.2011.03.009

Bogard, M. J., Kuhn, C. D., Johnston, S. E., Striegl, R. G., Holtgrieve, G. W., Dornblaser, M. M., & Butman, D. E. (2019). Negligible cycling of terrestrial carbon in many lakes of the arid circumpolar landscape. *Nature Geoscience*, *12*(3), 180–185. https://doi.org/10.1038/s41561-019-0299-5

Breton, J., Vallieres, C., & Laurion, I. (2009). Limnological properties of permafrost thaw ponds in northeastern Canada. *Canadian Journal of Fisheries and Aquatic Sciences*, *66*(10), 1635–1648. https://doi.org/10.1139/f09-108

Brown, J., Ferrians, O. J., Jr., Heginbottom, J. A., & Melnikov, E. S. (1997). *Circum-Arctic map of permafrost and ground-ice conditions* (p. 45). Reston, VA: US Geological Survey.

Coble, P. G. (1996). Characterization of marine and terrestrial DOM in seawater using excitation-emission matrix spectroscopy. *Marine Chemistry*, *51*(4), 325–346. https://doi.org/10.1016/0304-4203(95)00062-3

Cole, J. J., Prairie, Y. T., Caraco, N. F., McDowell, W. H., Tranvik, L. J., Striegl, R. G., & Melack, J. (2007). Plumbing the global carbon cycle: Integrating inland waters into the terrestrial carbon budget. *Ecosystems*, *10*(1), 172–185. https://doi.org/10.1007/s10021-006-9013-8

Collins, M., Knutti, R., Arblaster, J., Dufresne, J. L., Fichefet, T., Friedlingstein, P., et al. (2013). Long-term climate change: Projections, commitments and irreversibility. In *Climate Change 2013-The Physical Science Basis: Contribution of Working Group I to the Fifth Assessment Report of the Intergovernmental Panel on Climate Change* (pp. 1029–1136). Cambridge University Press.

Corilo, Y. E. (2014). *PetroOrg software*. Florida State University. All Rights reserved. Retrieved from http://www.petroorg.com

Cory, R. M., & McKnight, D. M. (2005). Fluorescence spectroscopy reveals ubiquitous presence of oxidized and reduced quinones in dissolved organic matter. *Environmental Science & Technology*, *39*(21), 8142–8149. https://doi.org/10.1021/es0506962

Cory, R. M., McKnight, D. M., Chin, Y. P., Miller, P., & Jaros, C. L. (2007). Chemical characteristics of fulvic acids from Arctic surface waters: Microbial contributions and photochemical transformations. *Journal of Geophysical Research: Biogeosciences*, *112*(G4). https://doi.org/10.1029/2006jg000343

Cory, R. M., Miller, M. P., McKnight, D. M., Guerard, J. J., & Miller, P. L. (2010). Effect of instrument-specific response on the analysis of fulvic acid fluorescence spectra. *Limnology and Oceanography: Methods*, *8*(2), 67–78. https://doi.org/10.4319/lom.2010.8.0067

D'Andrilli, J., Cooper, W. T., Foreman, C. M., & Marshall, A. G. (2015). An ultrahigh-resolution mass spectrometry index to estimate natural organic matter lability. *Rapid Communications in Mass Spectrometry*, *29*(24), 2385–2401. https://doi.org/10.1002/rcm.7400

del Giorgio, P. A., & Peters, R. H. (1994). Patterns in planktonic P: R ratios in lakes: Influence of lake trophy and dissolved organic carbon. *Limnology & Oceanography*, *39*(4), 772–787. https://doi.org/10.4319/lo.1994.39.4.0772

Denfeld, B. A., Baulch, H. M., delGiorgio, P. A., Hampton, S. E., & Karlsson, J. (2018). A synthesis of carbon dioxide and methane dynamics during the ice-covered period of northern lakes. *Limnology and Oceanography Letters*, *3*(3), 117–131. https://doi.org/10.1002/lol2.10079

Dittmar, T., Koch, B., Hertkorn, N., & Kattner, G. (2008). A simple and efficient method for the solid-phase extraction of dissolved organic matter (SPE-DOM) from seawater. *Limnology and Oceanography: Methods*, *6*(6), 230–235. https://doi.org/10.4319/lom.2008.6.230

Drake, T. W., Raymond, P. A., & Spencer, R. G. (2018). Terrestrial carbon inputs to inland waters: A current synthesis of estimates and uncertainty. *Limnology and Oceanography Letters*, *3*(3), 132–142. https://doi.org/10.1002/lol2.10055

Ducharme-Riel, V., Vachon, D., Del Giorgio, P. A., & Prairie, Y. T. (2015). The relative contribution of winter under-ice and summer hypolimnetic CO 2 accumulation to the annual CO2 emissions from northern lakes. *Ecosystems*, *18*(4), 547–559. https://doi.org/10.1007/s10021-015-9846-0

Dymond, C. C., & Johnson, E. A. (2002). Mapping vegetation spatial patterns from modeled water, temperature and solar radiation gradients. *ISPRS Journal of Photogrammetry and Remote Sensing*, *57*(1–2), 69–85. https://doi.org/10.1016/s0924-2716(02)00110-7

Elder, C. D., Xu, X., Walker, J., Schnell, J. L., Hinkel, K. M., Townsend-Small, A., & Czimczik, C. I. (2018). Greenhouse gas emissions from diverse Arctic Alaskan lakes are dominated by young carbon. *Nature Climate Change*, *8*(2), 166–171. https://doi.org/10.1038/s41558-017-0066-9

Fellman, J. B., Hood, E., & Spencer, R. G. (2010). Fluorescence spectroscopy opens new windows into dissolved organic matter dynamics in freshwater ecosystems: A review. *Limnology & Oceanography*, *55*(6), 2452–2462. https://doi.org/10.4319/lo.2010.55.6.2452

Frey, K. E., & McClelland, J. W. (2009). Impacts of permafrost degradation on arctic river biogeochemistry. *Hydrological Processes: International Journal*, *23*(1), 169–182. https://doi.org/10.1002/hyp.7196

Frey, K. E., Sobczak, W. V., Mann, P. J., & Holmes, R. M. (2016). Optical properties and bioavailability of dissolved organic matter along a flow-path continuum from soil pore waters to the Kolyma River mainstem, East Siberia. *Biogeosciences*, *13*(8), 2279–2290. https://doi.org/10.5194/bg-13-2279-2016

Gonsior, M., Schmitt-Kopplin, P., & Bastviken, D. (2013). Depth-dependent molecular composition and photo-reactivity of dissolved organic matter in a boreal lake under winter and summer conditions. *Biogeosciences*, *10*(11), 6945–6956. https://doi.org/10.5194/bg-10-6945-2013

Groeneveld, M., Catalán, N., Attermeyer, K., Hawkes, J., Einarsdóttir, K., Kothawala, D., & Tranvik, L. (2020). Selective adsorption of terrestrial dissolved organic matter to inorganic surfaces along a boreal inland water continuum. *Journal of Geophysical Research: Biogeosciences*, *125*(3), e2019JG005236. https://doi.org/10.1029/2019jg005236

Hampton, S. E., Moore, M. V., Ozersky, T., Stanley, E. H., Polashenski, C. M., & Galloway, A. W. (2015). Heating up a cold subject: Prospects for under-ice plankton research in lakes. *Journal of Plankton Research*, *37*(2), 277–284. https://doi.org/10.1093/plankt/fbv002

Hastie, A., Lauerwald, R., Weyhenmeyer, G., Sobek, S., Verpoorter, C., & Regnier, P. (2018). CO 2 evasion from boreal lakes: Revised estimate, drivers of spatial variability, and future projections. *Global Change Biology*, *24*(2), 711–728. https://doi.org/10.1111/gcb.13902

Hawkes, J. A., D'Andrilli, J., Agar, J. N., Barrow, M. P., Berg, S. M., Catalán, N., & Podgorski, D. C. (2020). An international laboratory comparison of dissolved organic matter composition by high resolution mass spectrometry: Are we getting the same answer? *Limnology and Oceanography: Methods*, *18*(6), 235–258. https://doi.org/10.1002/lom3.10364

Helms, J. R., Stubbins, A., Ritchie, J. D., Minor, E. C., Kieber, D. J., & Mopper, K. (2008). Absorption spectral slopes and slope ratios as indicators of molecular weight, source, and photobleaching of chromophoric dissolved organic matter. *Limnology & Oceanography*, *53*(3), 955–969. https://doi.org/10.4319/lo.2008.53.3.0955

Hinkel, K. M., Arp, C. D., Townsend-Small, A., & Frey, K. E. (2017). Can deep groundwater influx be detected from the geochemistry of thermokarst lakes in Arctic Alaska? *Permafrost and Periglacial Processes*, *28*(3), 552–557. https://doi.org/10.1002/ppp.1895

Hinkel, K. M., Eisner, W. R., Bockheim, J. G., Nelson, F. E., Peterson, K. M., & Dai, X. (2003). Spatial extent, age, and carbon stocks in drained thaw lake basins on the Barrow Peninsula, Alaska. *Arctic Antarctic and Alpine Research*, *35*(3), 291–300. https://doi.org/10.1657/1523-0430(2003)035[0291:seaacs]2.0.co;2

Hinkel, K. M., Frohn, R. C., Nelson, F. E., Eisner, W. R., & Beck, R. A. (2005). Morphometric and spatial analysis of thaw lakes and drained thaw lake basins in the Western Arctic Coastal Plain, Alaska. *Permafrost and Periglacial Processes*, *16*(4), 327–341. https://doi.org/10.1002/ppp.532

Hinkel, K. M., Lenters, J., Arp, C. D., & Frey, K. E. (2012). *Collaborative Research: Toward a Circumarctic lakes Observation Network (CALON)--Multiscale observations of lacustrine systems*. Arctic Data Center. https://doi.org/10.18739/A2VM42Z1H

Hinkel, K. M., Lenters, J. D., Sheng, Y., Lyons, E. A., Beck, R. A., Eisner, W. R., & Potter, B. L. (2012). Thermokarst lakes on the Arctic Coastal Plain of Alaska: Spatial and temporal variability in summer water temperature. *Permafrost and Periglacial Processes*, *23*(3), 207–217. https://doi.org/10.1002/ppp.1743

Hinkel, K. M., Lin, Z., Sheng, Y., & Lyons, E. A. (2012). Regional lake ice meltout patterns near Barrow, Alaska. *Polar Geography*, *35*(1), 1–18. https://doi.org/10.1080/1088937x.2011.654355

Jansen, J., MacIntyre, S., Barrett, D. C., Chin, Y. P., Cortés, A., Forrest, A. L., & Schwefel, R. (2021). Winter limnology: How do hydrodynamics and biogeochemistry shape ecosystems under ice? *Journal of Geophysical Research: Biogeosciences*, *126*(6), e2020JG006237. https://doi.org/10.1029/2020jg006237

Johnston, S. E., Bogard, M. J., Rogers, J. A., Butman, D., Striegl, R. G., Dornblaser, M., & Spencer, R. G. (2019). Constraining dissolved organic matter sources and temporal variability in a model sub-Arctic lake. *Biogeochemistry*, *146*(3), 271–292. https://doi.org/10.1007/s10533-019-00619-9

Johnston, S. E., Striegl, R. G., Bogard, M. J., Dornblaser, M. M., Butman, D. E., Kellerman, A. M., & Spencer, R. G. (2020). Hydrologic connectivity determines dissolved organic matter biogeochemistry in northern high-latitude lakes. *Limnology & Oceanography*, 1764–1780. https://doi.org/10.1002/lno.11417

Jones, B. M., Grosse, G. D. A. C., Arp, C. D., Jones, M. C., Anthony, K. W., & Romanovsky, V. E. (2011). Modern thermokarst lake dynamics in the continuous permafrost zone, northern Seward Peninsula, Alaska. *Journal of Geophysical Research*, *116*(G2). https://doi.org/10.1029/2011jg001666

Jorgenson, M. T., Shur, Y. L., & Pullman, E. R. (2006). Abrupt increase in permafrost degradation in Arctic Alaska. *Geophysical Research Letters*, *33*(2). https://doi.org/10.1029/2005gl024960

Kaiser, N. K., Quinn, J. P., Blakney, G. T., Hendrickson, C. L., & Marshall, A. G. (2011). A novel 9.4 Tesla FTICR mass spectrometer with improved sensitivity, mass resolution, and mass range. *Journal of the American Society for Mass Spectrometry*, *22*(8), 1343–1351. https://doi.org/10.1007/s13361-011-0141-9

Kassambara, A., & Mundt, F. (2017). Factoextra: Extract and visualize the results of multivariate data analyses. *R package version*, *1*(4), 2017

Kellerman, A. M., Dittmar, T., Kothawala, D. N., & Tranvik, L. J. (2014). Chemodiversity of dissolved organic matter in lakes driven by climate and hydrology. *Nature Communications*, *5*(1), 1–8. https://doi.org/10.1038/ncomms4804

Kellerman, A. M., Guillemette, F., Podgorski, D. C., Aiken, G. R., Butler, K. D., & Spencer, R. G. (2018). Unifying concepts linking dissolved organic matter composition to persistence in aquatic ecosystems. *Environmental Science & Technology*, *52*(5), 2538–2548. https://doi.org/10.1021/acs.est.7b05513

Kellerman, A. M., Hawkings, J. R., Wadham, J. L., Kohler, T. J., Stibal, M., Grater, E., & Spencer, R. G. M. (2020). Glacier outflow dissolved organic matter as a window into seasonally changing carbon sources: Leverett Glacier, Greenland. *Journal of Geophysical Research: Biogeosciences*, *125*(4), e2019JG005161. https://doi.org/10.1029/2019jg005161

Kind, T., & Fiehn, O. (2007). Seven Golden Rules for heuristic filtering of molecular formulas obtained by accurate mass spectrometry. *BMC Bioinformatics*, *8*(1), 1–20. https://doi.org/10.1186/1471-2105-8-105

Kling, G. W., Kipphut, G. W., & Miller, M. C. (1991). Arctic lakes and streams as gas conduits to the atmosphere: Implications for tundra carbon budgets. *Science*, *251*(4991), 298–301. https://doi.org/10.1126/science.251.4991.298

Koch, B. P., & Dittmar, T. (2006). From mass to structure: An aromaticity index for high-resolution mass data of natural organic matter. *Rapid Communications in Mass Spectrometry*, *20*(5), 926–932. https://doi.org/10.1002/rcm.2386

Koch, B. P., & Dittmar, T. (2016). From mass to structure: An aromaticity index for high-resolution mass data of natural organic matter. *Rapid Communications in Mass Spectrometry*, *30*, 250. https://doi.org/10.1002/rcm.7433

Koehler, B., Landelius, T., Weyhenmeyer, G. A., Machida, N., & Tranvik, L. J. (2014). Sunlight-induced carbon dioxide emissions from inland waters. *Global Biogeochemical Cycles*, *28*(7), 696–711. https://doi.org/10.1002/2014gb004850

Kothawala, D. N., Murphy, K. R., Stedmon, C. A., Weyhenmeyer, G. A., & Tranvik, L. J. (2013). Inner filter correction of dissolved organic matter fluorescence. *Limnology and Oceanography: Methods*, *11*(12), 616–630. https://doi.org/10.4319/lom.2013.11.616

Kurek, M. R., Harir, M., Shukle, J. T., Schroth, A. W., Schmitt-Kopplin, P., & Druschel, G. K. (2021). Seasonal transformations of dissolved organic matter and organic phosphorus in a polymictic basin: Implications for redox-driven eutrophication. *Chemical Geology*, *573*, 120212. https://doi.org/10.1016/j.chemgeo.2021.120212

Kurek, M. R., Poulin, B. A., McKenna, A. M., & Spencer, R. G. (2020). Deciphering dissolved organic matter: Ionization, dopant, and fragmentation insights via Fourier transform-ion cyclotron resonance mass spectrometry. *Environmental Science & Technology*, *54*(24), 16249–16259. https://doi.org/10.1021/acs.est.0c05206

Lambert, T., Teodoru, C. R., Nyoni, F. C., Bouillon, S., Darchambeau, F., Massicotte, P., & Borges, A. V. (2016). Along-stream transport and transformation of dissolved organic matter in a large tropical river. *Biogeosciences*, *13*(9), 2727–2741. https://doi.org/10.5194/bg-13-2727-2016

Lapierre, J. F., & Del Giorgio, P. A. (2014). Partial coupling and differential regulation of biologically and photochemically labile dissolved organic carbon across boreal aquatic networks. *Biogeosciences*, *11*(20), 5969–5985. https://doi.org/10.5194/bg-11-5969-2014

MacDonald, E. N., Tank, S. E., Kokelj, S. V., Froese, D. G., & Hutchins, R. H. (2021). Permafrost-derived dissolved organic matter composition varies across permafrost end-members in the Western Canadian Arctic. *Environmental Research Letters*, *16*(2), 024036. https://doi.org/10.1088/1748-9326/abd971

Mann, B. F., Chen, H., Herndon, E. M., Chu, R. K., Tolic, N., Portier, E. F., & Graham, D. E. (2015). Indexing permafrost soil organic matter degradation using high-resolution mass spectrometry. *PLoS One*, *10*(6), e0130557. https://doi.org/10.1371/journal.pone.0130557

Mann, P. J., Spencer, R. G., Hernes, P. J., Six, J., Aiken, G. R., Tank, S. E., & Holmes, R. M. (2016). Pan-Arctic trends in terrestrial dissolved organic matter from optical measurements. *Frontiers of Earth Science*, *4*, 25. https://doi.org/10.3389/feart.2016.00025

McGuire, A. D., Anderson, L. G., Christensen, T. R., Dallimore, S., Guo, L., Hayes, D. J., & Roulet, N. (2009). Sensitivity of the carbon cycle in the Arctic to climate change. *Ecological Monographs*, *79*(4), 523–555. https://doi.org/10.1890/08-2025.1

McKnight, D. M., Boyer, E. W., Westerhoff, P. K., Doran, P. T., Kulbe, T., & Andersen, D. T. (2001). Spectrofluorometric characterization of dissolved organic matter for indication of precursor organic material and aromaticity. *Limnology & Oceanography*, *46*(1), 38–48. https://doi.org/10.4319/lo.2001.46.1.0038

Michaelson, G. J., Ping, C. L., Kling, G. W., & Hobbie, J. E. (1998). The character and bioactivity of dissolved organic matter at thaw and in the spring runoff waters of the arctic tundra north slope, Alaska. *Journal of Geophysical Research: Atmospheres*, *103*(D22), 28939–28946. https://doi.org/10.1029/98jd02650

Murphy, K. R., Stedmon, C. A., Graeber, D., & Bro, R. (2013). Fluorescence spectroscopy and multi-way techniques. PARAFAC. *Analytical Methods*, *5*(23), 6557–6566. https://doi.org/10.1039/c3ay41160e

Natali, S. M., Watts, J. D., Rogers, B. M., Potter, S., Ludwig, S. M., Selbmann, A. K., & Zona, D. (2019). Large loss of CO2 in winter observed across the northern permafrost region. *Nature Climate Change*, *9*(11), 852–857. https://doi.org/10.1038/s41558-019-0592-8

Olefeldt, D., Goswami, S., Grosse, G., Hayes, D., Hugelius, G., Kuhry, P., & Turetsky, M. R. (2016). Circumpolar distribution and carbon storage of thermokarst landscapes. *Nature Communications*, *7*(1), 1–11. https://doi.org/10.1038/ncomms13043

Osburn, C. L., Anderson, N. J., Stedmon, C. A., Giles, M. E., Whiteford, E. J., McGenity, T. J., & Underwood, G. J. (2017). Shifts in the source and composition of dissolved organic matter in Southwest Greenland lakes along a regional hydro-climatic gradient. *Journal of Geophysical Research: Biogeosciences*, *122*(12), 3431–3445. https://doi.org/10.1002/2017jg003999

Peleato, N. M., Sidhu, B. S., Legge, R. L., & Andrews, R. C. (2017). Investigation of ozone and peroxone impacts on natural organic matter character and biofiltration performance using fluorescence spectroscopy. *Chemosphere*, *172*, 225–233. https://doi.org/10.1016/j.chemosphere.2016.12.118

Perminova, I. V., Dubinenkov, I. V., Kononikhin, A. S., Konstantinov, A. I., Zherebker, A. Y., Andzhushev, M. A., & Nikolaev, E. N. (2014). Molecular mapping of sorbent selectivities with respect to isolation of Arctic dissolved organic matter as measured by Fourier transform mass spectrometry. *Environmental Science & Technology*, *48*(13), 7461–7468. https://doi.org/10.1021/es5015423

Phelps, A. R., Peterson, K. M., & Jeffries, M. O. (1998). Methane efflux from high-latitude lakes during spring ice melt. *Journal of Geophysical Research: Atmospheres*, *103*(D22), 29029–29036. https://doi.org/10.1029/98jd00044

Poulin, B. A., Ryan, J. N., Nagy, K. L., Stubbins, A., Dittmar, T., Orem, W., & Aiken, G. R. (2017). Spatial dependence of reduced sulfur in Everglades dissolved organic matter controlled by sulfate enrichment. *Environmental Science & Technology*, *51*(7), 3630–3639. https://doi.org/10.1021/acs.est.6b04142

Rastelli, E., Corinaldesi, C., Dell'Anno, A., Martire, M. L., Greco, S., Facchini, M. C., & Danovaro, R. (2017). Transfer of labile organic matter and microbes from the ocean surface to the marine aerosol: An experimental approach. *Scientific Reports*, *7*(1), 1–10. https://doi.org/10.1038/s41598-017-10563-z

R Core Team. (2020). *R: A language and environment for statistical computing*. Vienna, Austria: R Foundation for Statistical Computing. Retrieved from https://www.R-project.org/

Santibáñez, P. A., Michaud, A. B., Vick-Majors, T. J., D'Andrilli, J., Chiuchiolo, A., Hand, K. P., & Priscu, J. C. (2019). Differential incorporation of bacteria, organic matter, and inorganic ions into lake ice during ice formation. *Journal of Geophysical Research: Biogeosciences*, *124*(3), 585–600

Schmitt-Kopplin, P., Liger-Belair, G., Koch, B. P., Flerus, R., Kattner, G., Harir, M., & Gebefügi, I. (2012). Dissolved organic matter in sea spray: A transfer study from marine surface water to aerosols. *Biogeosciences*, *9*(4), 1571–1582. https://doi.org/10.5194/bg-9-1571-2012

Schuur, E. A., McGuire, A. D., Schädel, C., Grosse, G., Harden, J. W., Hayes, D. J., & Vonk, J. E. (2015). Climate change and the permafrost carbon feedback. *Nature*, *520*(7546), 171–179. https://doi.org/10.1038/nature14338

Shatilla, N. J., & Carey, S. K. (2019). Assessing inter-annual and seasonal patterns of DOC and DOM quality across a complex alpine watershed underlain by discontinuous permafrost in Yukon, Canada. *Hydrology and Earth System Sciences*, *23*(9), 3571–3591. https://doi.org/10.5194/hess-23-3571-2019

Solomon, C. T., Jones, S. E., Weidel, B. C., Buffam, I., Fork, M. L., Karlsson, J., & Saros, J. E. (2015). Ecosystem consequences of changing inputs of terrestrial dissolved organic matter to lakes: Current knowledge and future challenges. *Ecosystems*, *18*(3), 376–389. https://doi.org/10.1007/s10021-015-9848-y

Spencer, R. G., Aiken, G. R., Butler, K. D., Dornblaser, M. M., Striegl, R. G., & Hernes, P. J. (2009). Utilizing chromophoric dissolved organic matter measurements to derive export and reactivity of dissolved organic carbon exported to the Arctic Ocean: A case study of the Yukon River, Alaska. *Geophysical Research Letters*, *36*(6). https://doi.org/10.1029/2008gl036831

Spencer, R. G., Aiken, G. R., Wickland, K. P., Striegl, R. G., & Hernes, P. J. (2008). Seasonal and spatial variability in dissolved organic matter quantity and composition from the Yukon River basin, Alaska. *Global Biogeochemical Cycles*, *22*(4). https://doi.org/10.1029/2008gb003231

Spencer, R. G., Bolton, L., & Baker, A. (2007). Freeze/thaw and pH effects on freshwater dissolved organic matter fluorescence and absorbance properties from a number of UK locations. *Water Research*, *41*(13), 2941–2950. https://doi.org/10.1016/j.watres.2007.04.012

Spencer, R. G., Mann, P. J., Dittmar, T., Eglinton, T. I., McIntyre, C., Holmes, R. M., & Stubbins, A. (2015). Detecting the signature of permafrost thaw in Arctic rivers. *Geophysical Research Letters*, *42*(8), 2830–2835. https://doi.org/10.1002/2015gl063498

Stackpoole, S. M., Butman, D. E., Clow, D. W., Verdin, K. L., Gaglioti, B. V., Genet, H., & Striegl, R. G. (2017). Inland waters and their role in the carbon cycle of Alaska. *Ecological Applications*, *27*(5), 1403–1420. https://doi.org/10.1002/eap.1552

Stedmon, C. A., Markager, S., & Bro, R. (2003). Tracing dissolved organic matter in aquatic environments using a new approach to fluorescence spectroscopy. *Marine Chemistry*, *82*(3–4), 239–254. https://doi.org/10.1016/s0304-4203(03)00072-0

Stedmon, C. A., Seredyńska-Sobecka, B., Boe-Hansen, R., LeTallec, N., Waul, C. K., & Arvin, E. (2011). A potential approach for monitoring drinking water quality from groundwater systems using organic matter fluorescence as an early warning for contamination events. *Water Research*, *45*(18), 6030–6038. https://doi.org/10.1016/j.watres.2011.08.066

Stubbins, A., Lapierre, J. F., Berggren, M., Prairie, Y. T., Dittmar, T., & delGiorgio, P. A. (2014). What's in an EEM? Molecular signatures associated with dissolved organic fluorescence in boreal Canada. *Environmental Science & Technology*, *48*(18), 10598–10606. https://doi.org/10.1021/es502086e

Stubbins, A., Spencer, R. G., Chen, H., Hatcher, P. G., Mopper, K., Hernes, P. J., & Six, J. (2010). Illuminated darkness: Molecular signatures of Congo River dissolved organic matter and its photochemical alteration as revealed by ultrahigh precision mass spectrometry. *Limnology & Oceanography*, *55*(4), 1467–1477. https://doi.org/10.4319/lo.2010.55.4.1467

Tank, S. E., Frey, K. E., Striegl, R. G., Raymond, P. A., Holmes, R. M., McClelland, J. W., & Peterson, B. J. (2012). Landscape-level controls on dissolved carbon flux from diverse catchments of the circumboreal. *Global Biogeochemical Cycles*, *26*(4). https://doi.org/10.1029/2012gb004299

Tank, S. E., Lesack, L. F., Gareis, J. A., Osburn, C. L., & Hesslein, R. H. (2011). Multiple tracers demonstrate distinct sources of dissolved organic matter to lakes of the Mackenzie Delta, Western Canadian Arctic. *Limnology & Oceanography*, *56*(4), 1297–1309. https://doi.org/10.4319/lo.2011.56.4.1297

Townsend-Small, A., Åkerström, F., Arp, C. D., & Hinkel, K. M. (2017). Spatial and temporal variation in methane concentrations, fluxes, and sources in lakes in Arctic Alaska. *Journal of Geophysical Research: Biogeosciences*, *122*(11), 2966–2981

Tranvik, L. J., Downing, J. A., Cotner, J. B., Loiselle, S. A., Striegl, R. G., Ballatore, T. J., & Kortelainen, P. L. (2009). Lakes and reservoirs as regulators of carbon cycling and climate. *Limnology & Oceanography*, *54*(6 Part 2), 2298–2314. https://doi.org/10.4319/lo.2009.54.6_part_2.2298

Vachon, D., Solomon, C. T., & delGiorgio, P. A. (2017). Reconstructing the seasonal dynamics and relative contribution of the major processes sustaining CO2 emissions in northern lakes. *Limnology & Oceanography*, *62*(2), 706–722. https://doi.org/10.1002/lno.10454

Valle, J., Gonsior, M., Harir, M., Enrich-Prast, A., Schmitt-Kopplin, P., Bastviken, D., & Hertkorn, N. (2018). Extensive processing of sediment pore water dissolved organic matter during anoxic incubation as observed by high-field mass spectrometry (FTICR-MS). *Water Research*, *129*, 252–263. https://doi.org/10.1016/j.watres.2017.11.015

Wang, J. J., Lafrenière, M. J., Lamoureux, S. F., Simpson, A. J., Gélinas, Y., & Simpson, M. J. (2018). Differences in riverine and pond water dissolved organic matter composition and sources in Canadian high Arctic watersheds affected by active layer detachments. *Environmental Science & Technology*, *52*(3), 1062–1071. https://doi.org/10.1021/acs.est.7b05506

Wauthy, M., Rautio, M., Christoffersen, K. S., Forsström, L., Laurion, I., Mariash, H. L., & Vincent, W. F. (2018). Increasing dominance of terrigenous organic matter in circumpolar freshwaters due to permafrost thaw. *Limnology and Oceanography Letters*, *3*(3), 186–198. https://doi.org/10.1002/lol2.10063

Weishaar, J. L., Aiken, G. R., Bergamaschi, B. A., Fram, M. S., Fujii, R., & Mopper, K. (2003). Evaluation of specific ultraviolet absorbance as an indicator of the chemical composition and reactivity of dissolved organic carbon. *Environmental Science & Technology*, *37*(20), 4702–4708. https://doi.org/10.1021/es030360x

Wendler, G., Gordon, T., & Stuefer, M. (2017). On the precipitation and precipitation change in Alaska. *Atmosphere*, *8*(12), 253. https://doi.org/10.3390/atmos8120253

Wickham, H. (2016). *ggplot2: Elegant graphics for data analysis*. Springer.

Wickland, K. P., Aiken, G. R., Butler, K., Dornblaser, M. M., Spencer, R. G. M., & Striegl, R. G. (2012). Biodegradability of dissolved organic carbon in the Yukon River and its tributaries: Seasonality and importance of inorganic nitrogen. *Global Biogeochemical Cycles*, *26*(4). https://doi.org/10.1029/2012gb004342

Wologo, E., Shakil, S., Zolkos, S., Textor, S., Ewing, S., Klassen, J., & Abbott, B. W. (2021). Stream dissolved organic matter in permafrost regions shows surprising compositional similarities but negative priming and nutrient effects. *Global Biogeochemical Cycles*, *35*(1), e2020GB006719. https://doi.org/10.1029/2020gb006719

Woods, G. C., Simpson, M. J., Pautler, B. G., Lamoureux, S. F., Lafrenière, M. J., & Simpson, A. J. (2011). Evidence for the enhanced lability of dissolved organic matter following permafrost slope disturbance in the Canadian High Arctic. *Geochimica et Cosmochimica Acta*, *75*(22), 7226–7241. https://doi.org/10.1016/j.gca.2011.08.013

Wünsch, U. J., Murphy, K. R., & Stedmon, C. A. (2017). The one-sample PARAFAC approach reveals molecular size distributions of fluorescent components in dissolved organic matter. *Environmental Science & Technology*, *51*(20), 11900–11908

Yamashita, Y., Panton, A., Mahaffey, C., & Jaffé, R. (2011). Assessing the spatial and temporal variability of dissolved organic matter in Liverpool Bay using excitation–emission matrix fluorescence and parallel factor analysis. *Ocean Dynamics*, *61*(5), 569–579. https://doi.org/10.1007/s10236-010-0365-4

Zhang, T., Osterkamp, T. E., & Stamnes, K. (1996). Some characteristics of the climate in northern Alaska, USA. *Arctic and Alpine Research*, *28*(4), 509–518. https://doi.org/10.2307/1551862

Zherebker, A., Kim, S., Schmitt-Kopplin, P., Spencer, R. G., Lechtenfeld, O., Podgorski, D. C., & Perminova, I. V. (2020). Interlaboratory comparison of humic substances compositional space as measured by Fourier transform ion cyclotron resonance mass spectrometry (IUPAC Technical Report). *Pure and Applied Chemistry*, *1*. https://doi.org/10.1515/pac-2019-0809

Zhou, Y., Martin, P., & Müller, M. (2019). Composition and cycling of dissolved organic matter from tropical peatlands of coastal Sarawak, Borneo, revealed by fluorescence spectroscopy and parallel factor analysis. *Biogeosciences*, *16*(13), 2733–2749. https://doi.org/10.5194/bg-16-2733-2019